

9325  
RI

**RI 9325**

**REPORT OF INVESTIGATIONS/1990**

PLEASE DO NOT REMOVE FROM LIBRARY

National Institute for  
Occupational Safety & Health  
Spokane Research Center  
E. 415 Montgomery Ave.  
Spokane, WA 99207  
Library

# Mitigating Destructive Longwall Bumps Through Conventional Gate Entry Design

By Alan A. Campoli, Timothy M. Barton, Fred C. Van Dyke,  
and Michael Gauna

1910 ★ **80** ★ 1990  
YEARS

**BUREAU OF MINES**



**UNITED STATES DEPARTMENT OF THE INTERIOR**

U.S. Bureau of Mines  
Spokane Research Center  
E. 315 Montgomery Ave.  
Spokane, WA 99207  
**LIBRARY**

National Institute for  
Occupational Safety & Health  
Spokane Research Center  
E. 315 Montgomery Ave.  
Spokane, WA 99207  
**Library**

**Mission:** As the Nation's principal conservation agency, the Department of the Interior has responsibility for most of our nationally-owned public lands and natural and cultural resources. This includes fostering wise use of our land and water resources, protecting our fish and wildlife, preserving the environmental and cultural values of our national parks and historical places, and providing for the enjoyment of life through outdoor recreation. The Department assesses our energy and mineral resources and works to assure that their development is in the best interests of all our people. The Department also promotes the goals of the Take Pride in America campaign by encouraging stewardship and citizen responsibility for the public lands and promoting citizen participation in their care. The Department also has a major responsibility for American Indian reservation communities and for people who live in Island Territories under U.S. Administration.

**Report of Investigations 9325**

# **Mitigating Destructive Longwall Bumps Through Conventional Gate Entry Design**

**By Alan A. Campoli, Timothy M. Barton, Fred C. Van Dyke,  
and Michael Gauna**

**UNITED STATES DEPARTMENT OF THE INTERIOR  
Manuel Lujan, Jr., Secretary**

**BUREAU OF MINES  
T S Ary, Director**

**Library of Congress Cataloging in Publication Data:**

Mitigating destructive longwall bumps through conventional gate entry design / by  
Alan A. Campoli ...[et al.].

p. cm. — (Report of investigations; 9325)

Supt. of Docs. no.: I 28.23:9325.

1. Mine roof control. 2. Rock bursts. 3. Longwall mining. I. Campoli, A. A.  
(Alan A.) II. Series.

TN23.U43 [TN288] 622 s—dc20 [622'.334] 90-2082 CIP

## CONTENTS

	<i>Page</i>
Abstract .....	1
Introduction .....	2
Acknowledgments .....	2
Geologic setting .....	2
Qualitative evaluation of gate entry system performance .....	11
Bump events in 6 and 7 development .....	12
Ground control experience in 8 development .....	15
Quantitative evaluation of gate entry system performance .....	22
Borehole platened flatjack .....	22
Coalbed stress in 7 development .....	24
Mining of panel S-6 .....	24
Mining of panel S-7 .....	25
Coalbed stress in 8 development .....	25
Mining of panel S-7 .....	25
Mining of panel S-8 .....	26
Average weighted coalbed stress .....	27
Abutment pillar dilation .....	28
Mining-induced roof and floor deformation .....	31
Roof-to-floor convergence .....	31
Immediate roof and floor strata separation .....	33
Summary and conclusions .....	34
References .....	35
Appendix.—Data acquisition system description and operation .....	36

## ILLUSTRATIONS

1. Study area location map .....	3
2. Mine map .....	3
3. Generalized stratigraphic column for study area .....	4
4. Overburden map for Pocahontas No. 3 Coalbed .....	5
5. Structure contour map on base of Pocahontas No. 3 Coalbed .....	6
6. Siltstone immediate roof thickness map .....	7
7. Quartzite sandstone main roof thickness map .....	8
8. Lithographic log and physical properties data for immediate roof over Pocahontas No. 3 Coalbed .....	9
9. Lithographic log and physical properties data for immediate floor and Pocahontas No. 3 Coalbed .....	10
10. Superjacent strata conditions over 6, 7, and 8 development gate entry systems .....	11
11. Plan view of bump A within 6 development gate entry system .....	13
12. Typical tailgate crib support configuration in 6 and 7 development gate entry systems .....	14
13. Plan view of bump C within 7 development gate entry system .....	15
14. Condition of crosscut between pillars E and F and crosscut between pillars F and G .....	16
15. Plan view of conditions at site F, within 8 development detailed study area .....	17
16. Conditions within 8 development detailed study area .....	18
17. Map of 7 development instrument array .....	22
18. Map of 8 development instrument array .....	23
19. Borehole platened flatjack configuration .....	23
20. Borehole platened flatjack installation procedure .....	23
21. Coalbed stress change in 7 development study area during mining of panel S-6 .....	24
22. Coalbed stress change across 7 development abutment pillars during mining of panel S-7 .....	25
23. Coalbed stress change in 8 development study area during mining of panel S-7 .....	26
24. Coalbed stress change across edge of panel S-7 during mining of panel S-7 .....	26
25. Coalbed stress change across edge of panel S-8 during mining of panel S-7 .....	27

**ILLUSTRATIONS—continued**

	<i>Page</i>
26. Coalbed stress change across 8 development abutment pillars during mining of panel S-8 . . . . .	27
27. Coalbed stress change across edge of panel S-8 during mining of panel S-8 . . . . .	28
28. Averaged weighted coalbed stress change in head and tail yield pillars during headgate panel mining . . .	28
29. Averaged weighted coalbed stress change in abutment pillars during headgate and tailgate panel mining .	29
30. Strain in perimeter of 7 development abutment pillars during mining of panel S-6 . . . . .	29
31. Strain recorded in extensometer 1 in 7 development abutment pillar during panel S-7 mining . . . . .	30
32. Strain in perimeter of 8 development abutment pillars during mining of panel S-7 . . . . .	30
33. Strain recorded in extensometer 1 in 8 development abutment pillar during panel S-8 mining . . . . .	30
34. Roof-to-floor convergence measurement with portable, telescoping rod . . . . .	31
35. String pot potentiometer, remote reading, roof-to-floor convergence sensor assembly . . . . .	32
36. Roof-to-floor convergence across 7 development cross section during mining of panel S-6 and panel S-7 .	32
37. Roof-to-floor convergence across 8 development cross section during mining of panel S-7 and panel S-8 .	33
38. Roof separation and bottom heave induced in center of 8 development instrument array . . . . .	33
A-1. Data acquisition system configuration . . . . .	36
A-2. Underground examination of voltage-to-frequency card, attached to transducer-equipped borehole platened flatjack . . . . .	37
A-3. Underground examination of field data station and associated equipment . . . . .	37

**UNIT OF MEASURE ABBREVIATIONS USED IN THIS REPORT**

A	ampere	mA	milliampere
ft	foot	pct	percent
Hz	hertz	psi	pound (force) per square inch
in	inch	V ac	volt, alternating current
in/in	inch per inch (strain)	V dc	volt, direct current

# MITIGATING DESTRUCTIVE LONGWALL BUMPS THROUGH CONVENTIONAL GATE ENTRY DESIGN

By Alan A. Campoli,<sup>1</sup> Timothy M. Barton,<sup>1</sup> Fred C. Van Dyke,<sup>2</sup> and Michael Gauna<sup>3</sup>

---

## ABSTRACT

The U.S. Bureau of Mines evaluated two different conventional longwall gate entry systems in the Southern Appalachian Basin, where mining and geologic conditions are conducive for coal pillar bumps. These gate entry systems were in a coal mine located in the Pocahontas No. 3 Coalbed under approximately 2,000 ft of overburden and a massive quartzite sandstone member, and both employed a center abutment pillar flanked by yield pillars. The 80-ft-square tailgate abutment pillars within the first study area began bumping 500 ft in advance of mining. This was accompanied by face bumps on the tailgate corner of the longwall face. The 120- by 180-ft tailgate abutment pillars within the second study area did not begin to bump until mining was approximately 100 ft past. Coalbed stress change and abutment pillar dilation data demonstrated that a 15-ft-wide perimeter of yielded coal surrounded a highly stressed core in both sizes of abutment pillars. The 62 pct more core area per foot of gate entry in the larger abutment pillars prevented excessive load transfer to the corner of the tailgate panel and eliminated the face bumps experienced with the original gate entry design.

---

<sup>1</sup>Mining engineer, Pittsburgh Research Center, U.S. Bureau of Mines, Pittsburgh, PA.

<sup>2</sup>Mining engineering technician, Pittsburgh Research Center.

<sup>3</sup>Manager, Planning Engineering, Island Creek Coal Co., Oakwood, VA.

## INTRODUCTION

Full-extraction retreat coal mining concentrates stress in the coal adjacent to expanding gob areas. When mining is conducted at great depth and between rigid roof and floor strata, highly stressed portions of coal pillars often fail violently. These "bumps" vary from minor vibrations without significant strata movement to notable earth tremors with thousands of tons of coal ejected into the mine workings.

The Southern Appalachian Basin of the United States has had a long history of coal bumps and bump-related research. One of the earliest detailed reports about coal bumps in this area was compiled by Rice (1).<sup>4</sup> This 1935 report identified numerous sites of coal pillar bumps in eastern Kentucky and southwestern Virginia, and noted that in one 4-month period, eight miners were killed and a number injured by bumps. In another report, Holland (2) examined 177 instances of pillar bumps, most of which were in the Southern Appalachian Basin, and found that the primary cause of these bumps was "unfavorable" mining practices in abutment areas. Talman (3) noted the importance of very stiff overlying strata to the occurrence of bumps, thereby emphasizing the influence of local geologic conditions. Comprehensive laboratory and field data on the physical properties of two bump-prone coals from southern Appalachia (the Pocahontas No. 3 and No. 4) were reported by Wang (4).

The U.S. Bureau of Mines reinitiated coal mine bump research in the Southern Appalachian Basin because of a rash of bump-related fatalities and injuries in 1984 and 1985 (5). A preliminary investigation of the geologic, mining, and engineering parameters at five sites in West Virginia and Virginia, where recent miner fatalities or injuries were associated with coal bumps, confirmed that stiff, competent associated strata and the high stresses

generated by retreat mining were common to all five sites. Campoli (5) recommended, as did Holland before him, that mine designs should avoid the development of pillar line points or long roof spans, which propagate bumps. Also, retreating longwalls with carefully designed gate entry systems were recommended over room-and-pillar retreat in bump-prone mines, because of the increased extraction rates and enhanced bump control associated with retreating longwalls (5).

The long-term objective of the Bureau's fundamental studies of coal mine bumps is to develop a design criterion that can be used to minimize the bump hazard of mining layouts. The foundation of this program is the delineation of the detailed reactions and physical properties of the bump-prone coal strata through in-mine evaluations. The program began with an in-mine evaluation of a novel extraction sequence used to control bumps during room-and-pillar retreat coal mining at the Olga Mine, McDowell County, WV (6). This novel retreat mining system, which mined over three pillar rows outby the gob, distributed abutment loads up to six pillar rows outby the newly formed gob. Microseismic monitoring was also conducted in the Olga Mine study area, and the results of this effort were reported by Condon (7). The results of the Olga Mine study have been enhanced by an evaluation of two different longwall gate entry configurations in a bump-prone coal mine in the Southern Appalachian Basin. The effect of increased abutment pillar size on gate entry stability and bump occurrence was evaluated through two detailed instrument arrays, rock property testing, and in-mine observations. This effort was necessary because of the lack of understanding of pillar failure mechanisms and longwall abutment load transfer under bump-prone conditions.

## ACKNOWLEDGMENTS

This work could not have been accomplished without the help of many Island Creek Coal Co. employees well acquainted with coal mine bumps. Kenneth R. Price, general manager, Rufus Fox, operations manager, Eddie Ball, mine superintendent, and Howard Epperly, manager of

engineering, all from the Virginia Pocahontas Division, Oakwood, VA, provided the valued information, insight, advice, and in-mine assistance that made this publication possible.

## GEOLOGIC SETTING

The study area is located in Buchanan County, VA (fig. 1). A total of 16 longwall panels have been mined

from the subject mine (fig. 2). Eight successive panels have been mined both to the north and south of twin barrier pillars. The gate entry system between the sixth and seventh panels to the south contained what will be referred to as the "7 development" study area. It was the

<sup>4</sup>Italic numbers in parentheses refer to items in the list of references preceding the appendix at the end of this report.

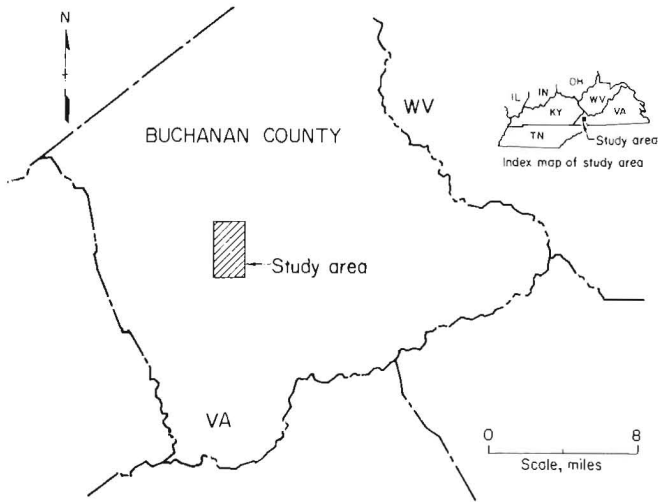


Figure 1.—Study area location map.

site of the first of two detailed instrument arrays, the locations of which are indicated on figure 2. The "8 development" study area was located between the seventh and eighth panels to the south.

The mine extracts the Pocahontas No. 3 Coalbed, which is located in the Pocahontas Formation and averages 5.5 ft in thickness (fig. 3). Minewide, the Pocahontas No. 3 Coalbed is under overburden ranging from 1,200 to 2,200 ft in thickness (fig. 4) and dips gradually from east to west (fig. 5). The immediate roof in the south end of the mine consists of a widely jointed siltstone overlain by a massive quartz arenite sandstone. Minewide, the siltstone ranges from a maximum thickness of 110 ft to being nonexistent (fig. 6). The massive quartz arenite sandstone ranges from a maximum thickness of 450 to a minimum of 135 ft over the mine (fig. 7). The mine floor in the south end of the mine consists of a combination of very competent siltstone and sandstone.

Underground observations in the study area, reported by Iannacchione (8), indicate that there is a persistent absence of prominent roof and floor fractures or joints and that the main roof, dominated by the thick quartz arenite sandstone, is exceedingly difficult to break. These unique geologic conditions apparently cause greater pillar loads in the study area than would be predicted by conventional, empirical abutment load calculations, such as those proposed by Mark (9).

The Bureau's borehole deformation gauge was used in a vertical corehole drilled into the roof above the Pocahontas No. 3 Coalbed to measure the horizontal components of in situ roof stress. The hole was drilled in the center of the 8 development study area (fig. 2). The average horizontal principal stresses were determined to be

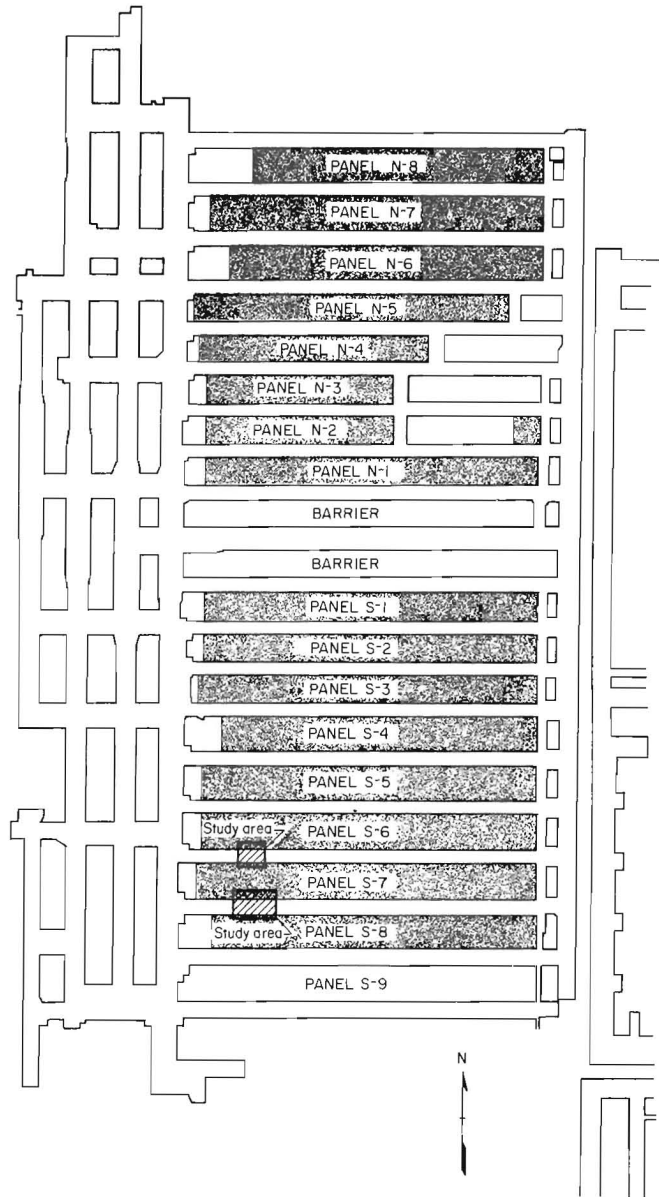


Figure 2.—Mine map.

-3,400 psi at N 76° E and -1,590 psi at N 16° W, by the anisotropic method described by Hooker (10).

These values are similar to borehole deformation gauge results obtained between 1978 and 1980 by Tosco Research, Inc., under a contract with the Bureau (11) and by the Bureau at the Olga Mine, during the aforementioned room-and-pillar bump research (6). The Tosco measurements were taken in rock above the Beckley Coalbed. Close agreement found in both the magnitude and direction of the horizontal in situ roof stresses above the Beckley, Pocahontas No. 4, and Pocahontas No. 3

Coalbeds suggests that the stresses measured at all of these sites were produced by regional tectonics. Oylar (12) suggested that since the mines studied by Tosco were not noted for having bump problems, horizontal stress did not contribute to the bump problems in southern West Virginia. This assumption now can be extended to the Pocahontas No. 3 Coalbed, based on the in situ horizontal roof stress results from 8 development.

NX-size coreholes were drilled 42 ft into the immediate roof and 32 ft into the immediate floor in the center of the 8 development study area. Detailed lithologic logs were produced from visual examination of the recovered core.

Unconfined compressive and Brazilian tensile tests were performed on selected core samples, and Young's moduli and Poisson ratios for the rock were calculated. The lithologic logs and the physical properties of the immediate roof and floor are presented in figures 8 and 9, respectively (13). The strength and stiffness of the strata surrounding the Pocahontas No. 3 Coalbed in the study area are uncommonly high for coal measure rocks. Similarly, high strength and stiffness properties were reported by Iannacchione (14) for the strata surrounding the Pocahontas No. 4 Coalbed in bump-prone areas.

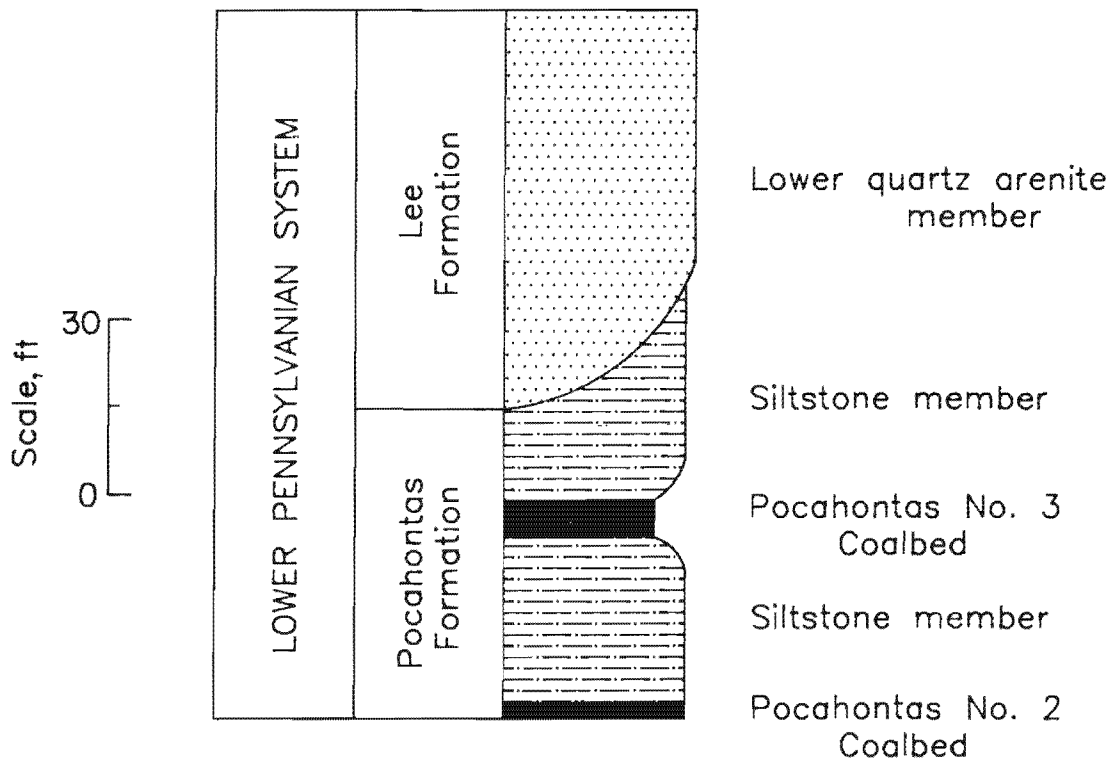


Figure 3.—Generalized stratigraphic column for study area.

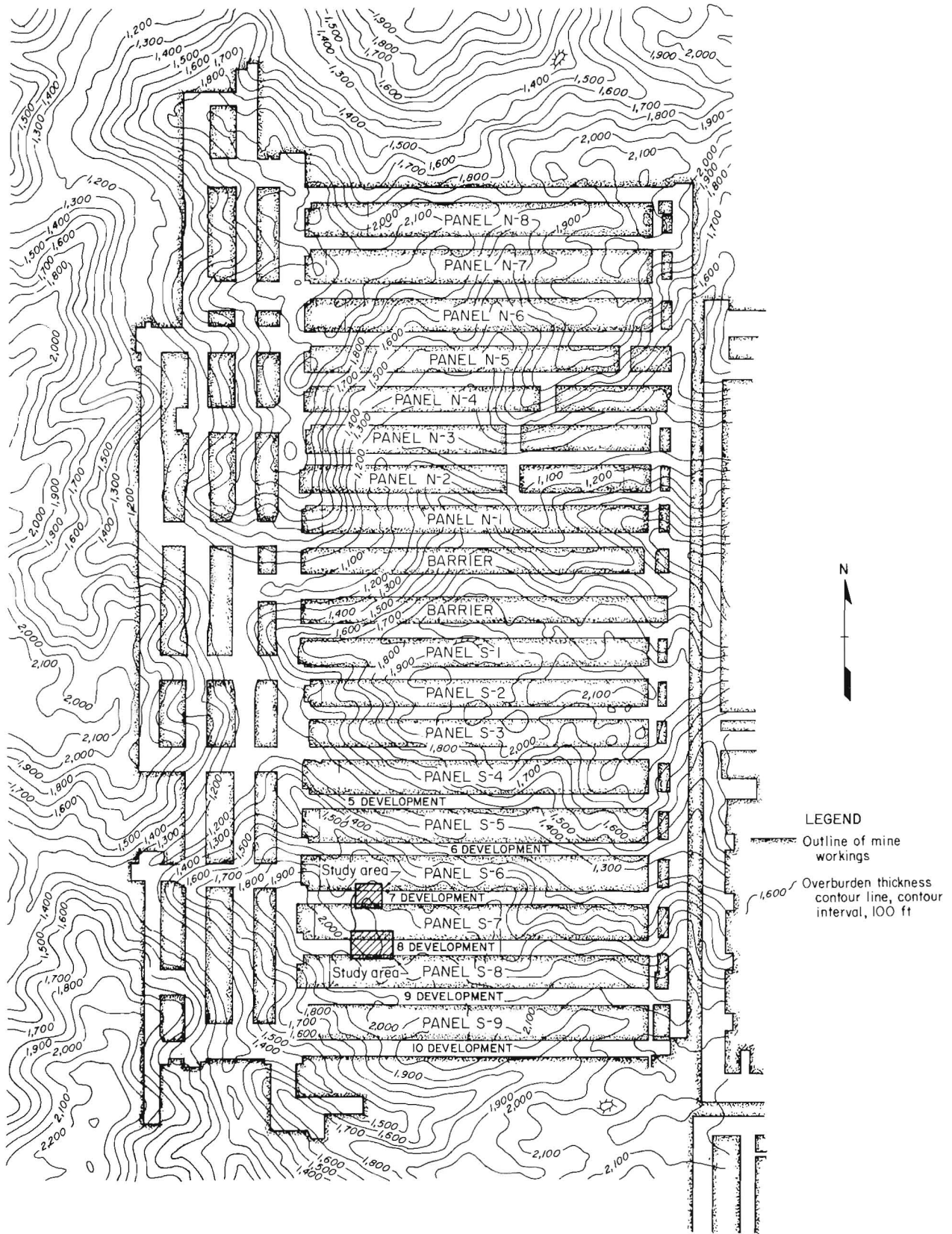


Figure 4.—Overburden map for Pocahontas No. 3 Coalbed.

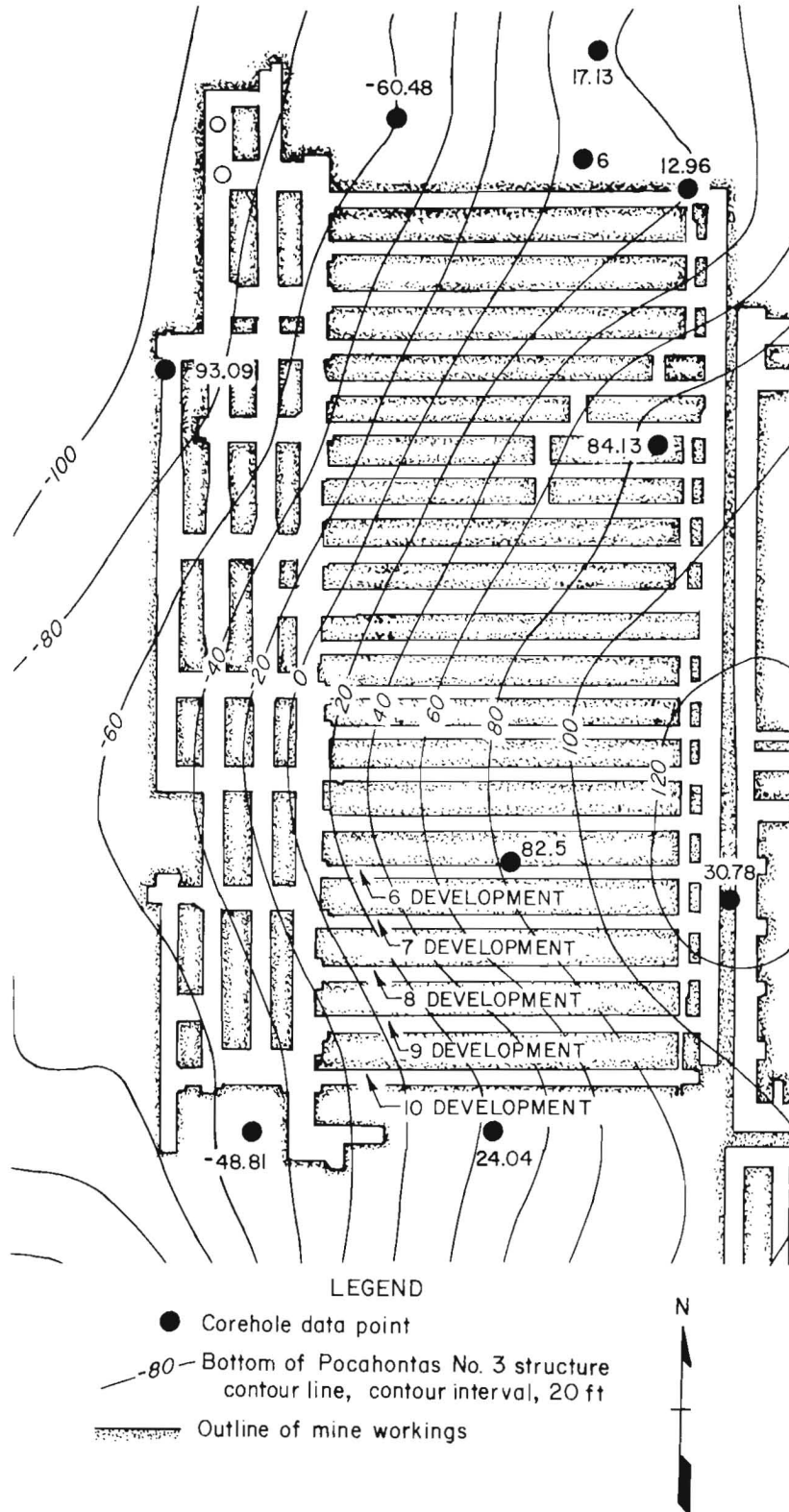


Figure 5.—Structure contour map on base of Pocahontas No. 3 Coalbed.

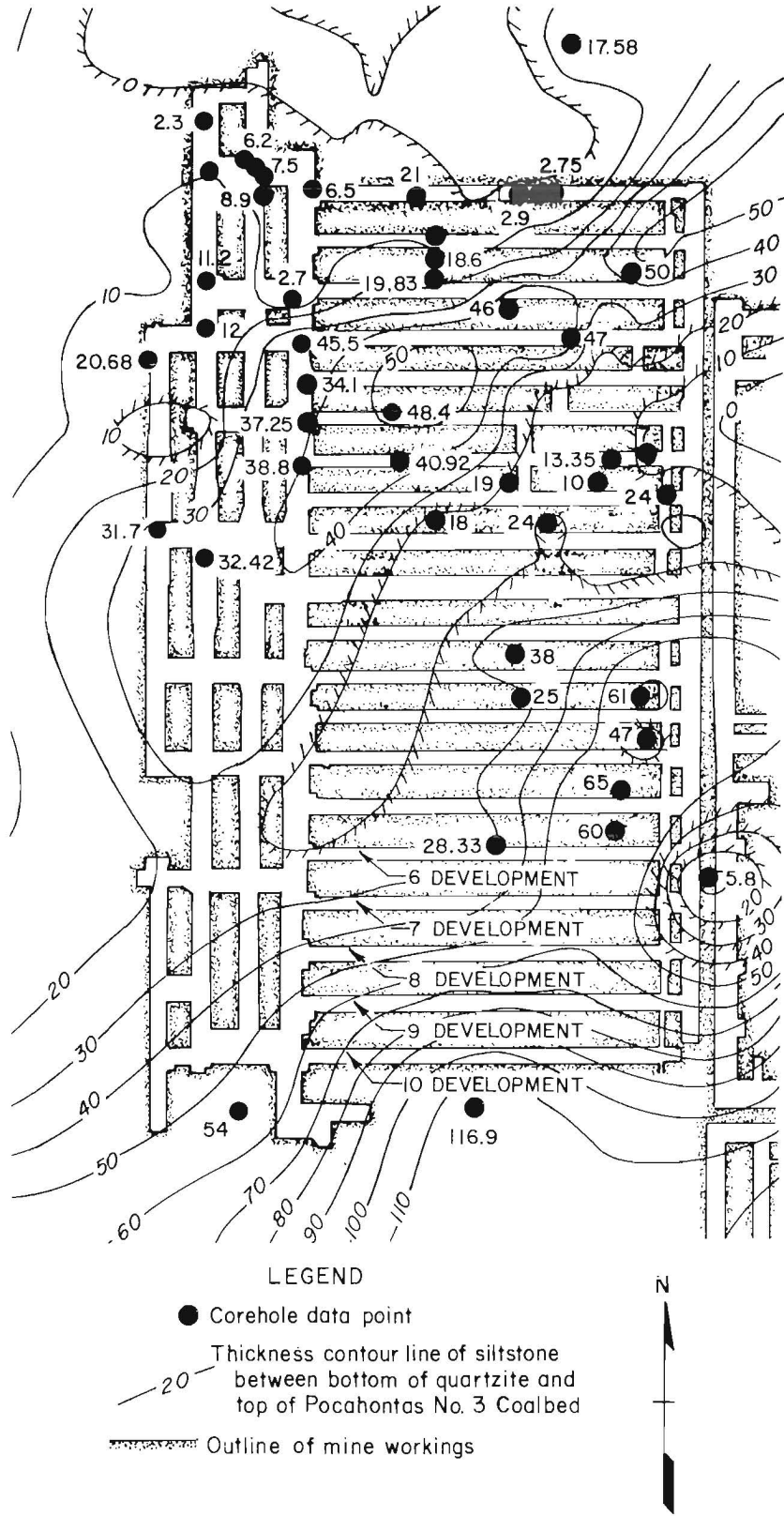


Figure 6.—Siltstone immediate roof thickness map.

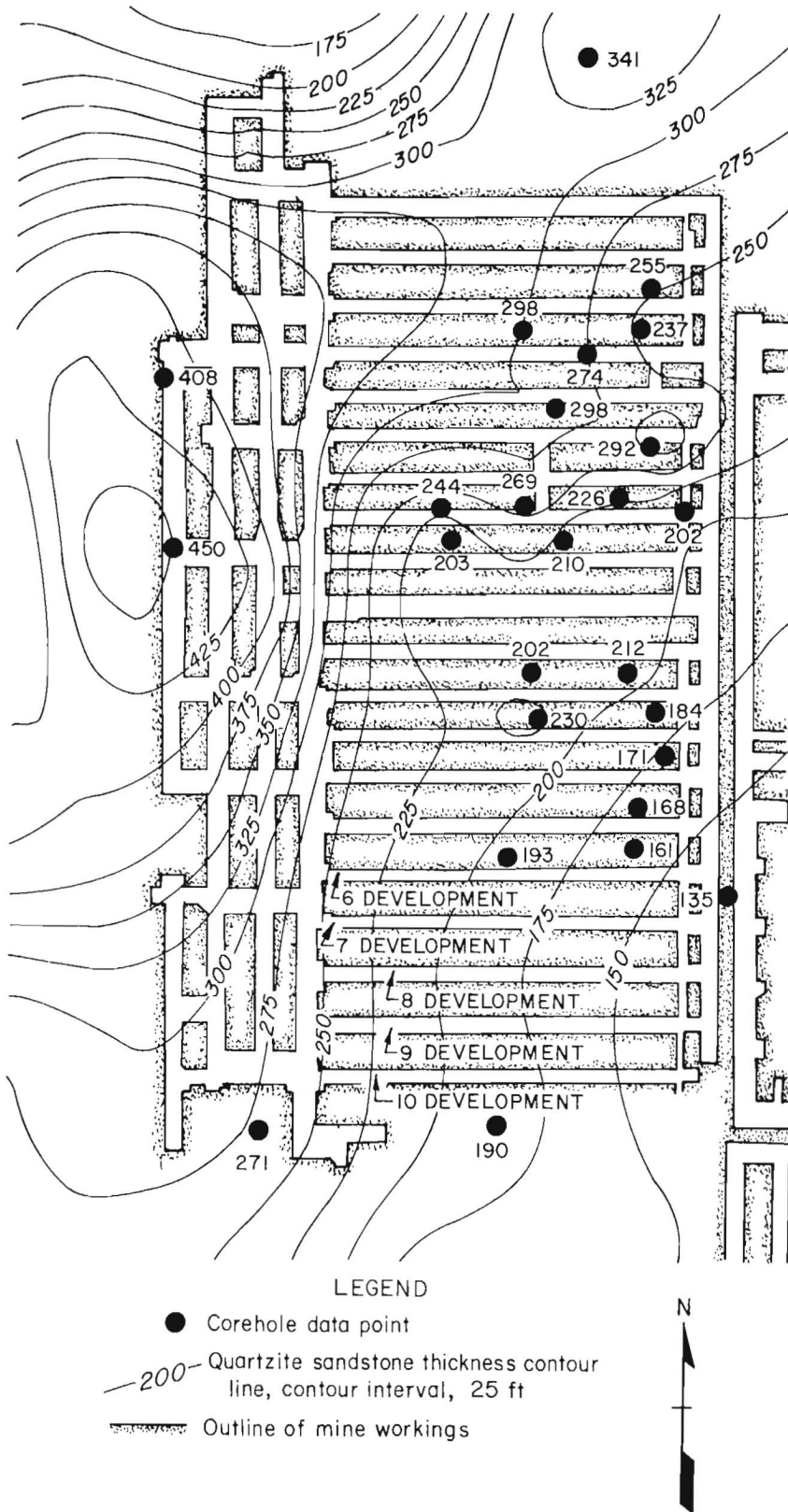
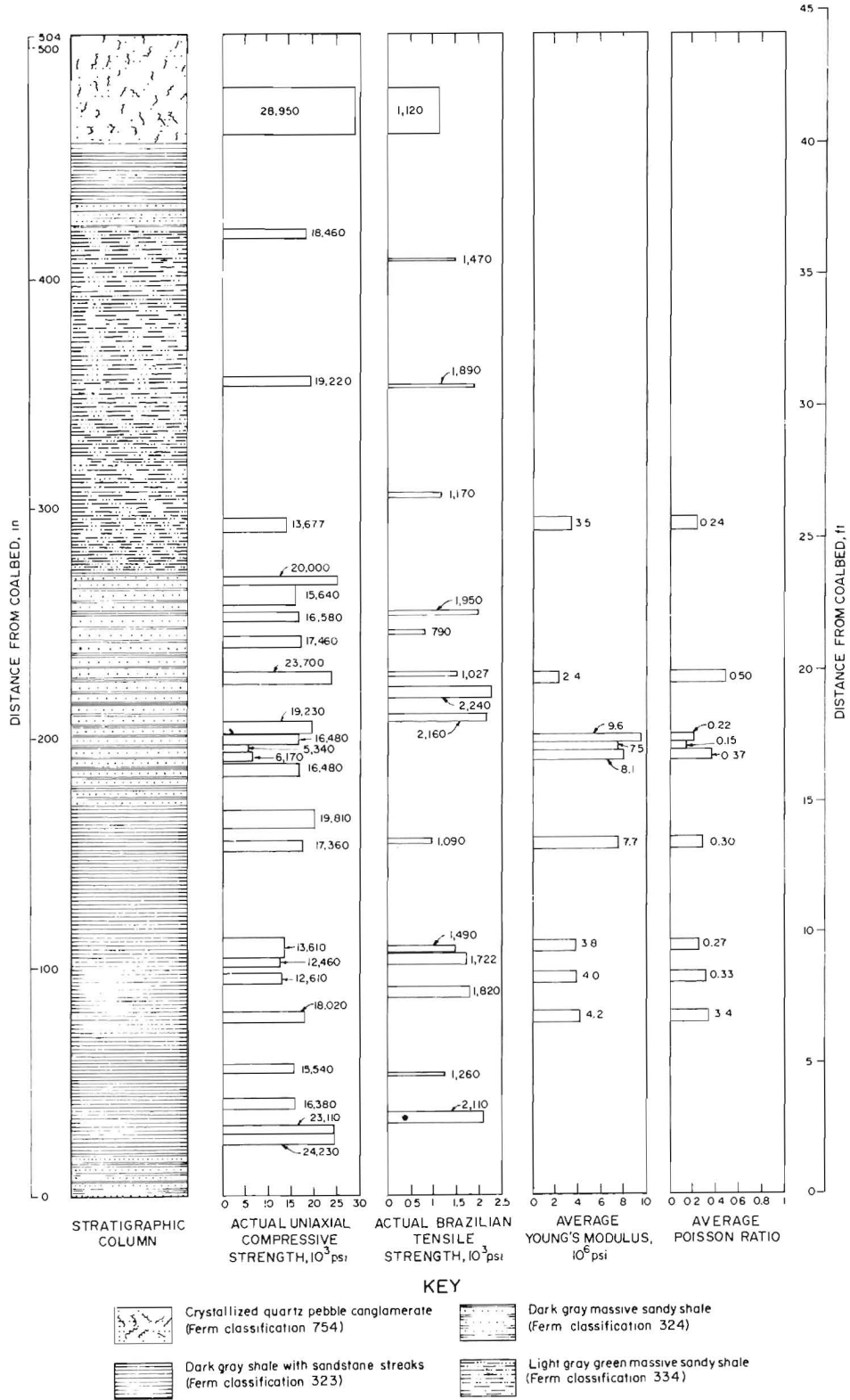
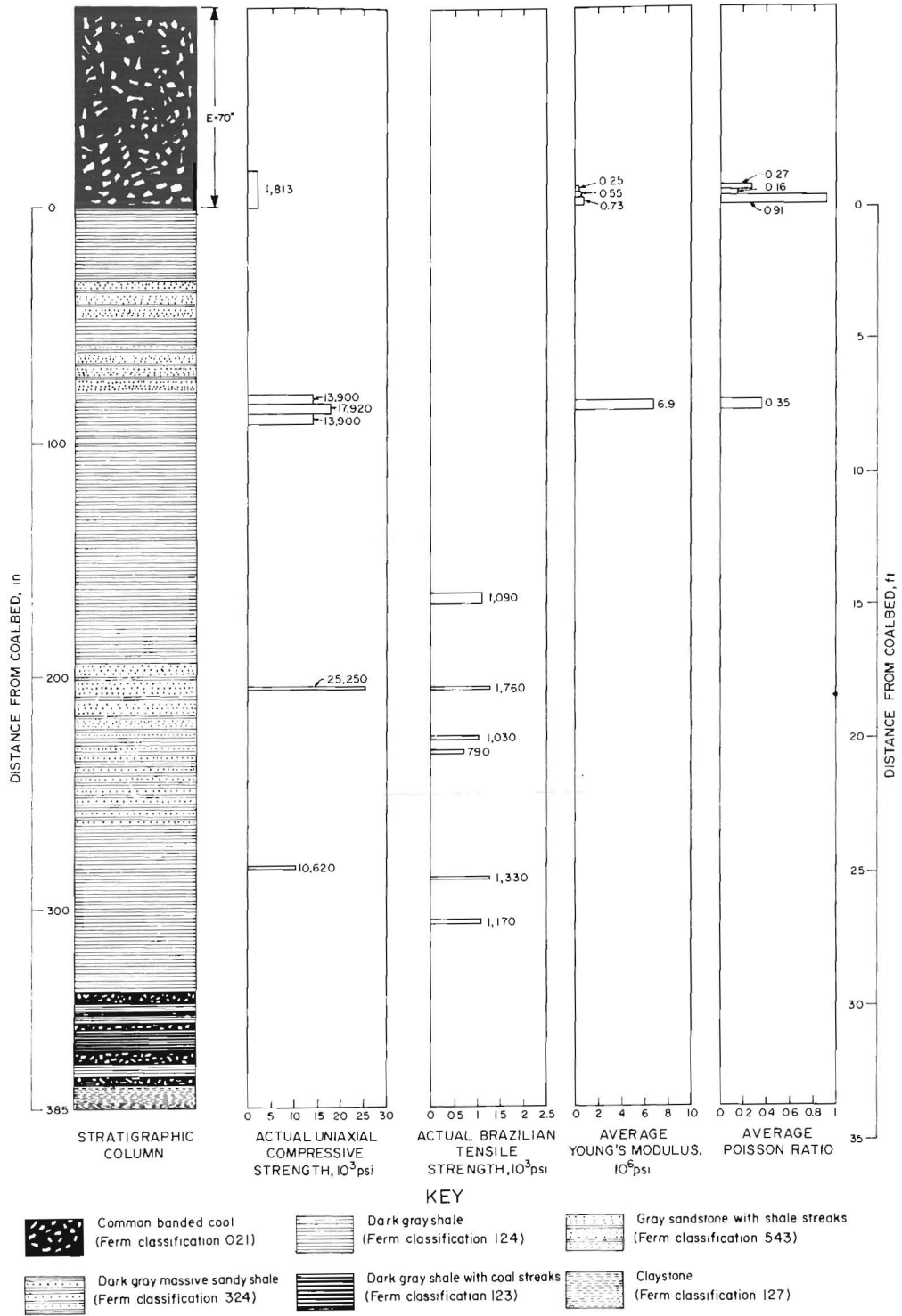


Figure 7.—Quartzite sandstone main roof thickness map.



**Figure 8.—Lithographic log and physical properties data for immediate roof over Pocahontas No. 3 Coalbed.**



**Figure 9.—Lithographic log and physical properties data for Immediate floor and Pocahontas No. 3 Coalbed.**

### QUALITATIVE EVALUATION OF GATE ENTRY SYSTEM PERFORMANCE

A section of the mine plan showing the 6, 7, and 8 development gate entry systems is presented in figure 10. All of the gate entry systems in this mine are of a conventional design. Conventional designs are intended to support a major portion of the abutment load resulting from adjacent gob formation. This is in contrast to an all-yeild design that immediately transfers abutment load to the longwall panel during adjacent panel mining. Figure 10 also displays the variations in the overburden, siltstone immediate roof, and quartzite main roof thicknesses directly above the 6, 7, and 8 development gate entry systems. Panels S-5, S-6, S-7, and S-8 are roughly 600 ft wide and

6,000 ft long. The first detailed study area, located in the 7 development gate entry system, is centered approximately 4,700 ft from the startup entry of panel S-6, under approximately 1,950 ft of overburden. The second detailed study area, in the 8 development gate entry system, is centered approximately 4,600 ft from the start-up entry of panel S-7, under approximately 2,050 ft of overburden. Thus, the two study areas are located adjacent to each other on opposite sides of panel S-7. This juxtaposition of these two conventional, but strategically different gate entry system designs in highly stressed strata provided a unique opportunity for obtaining a better understanding of

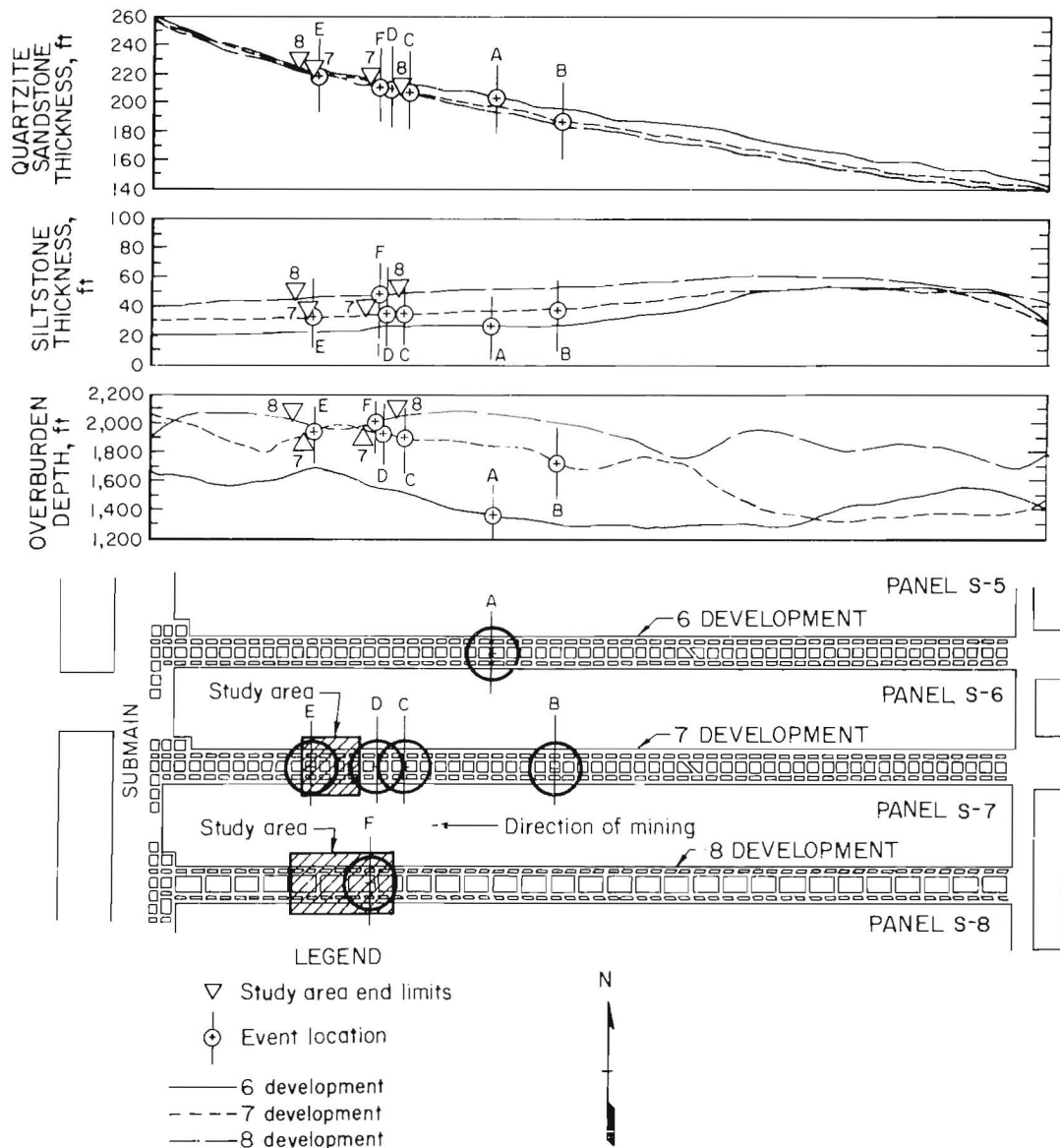


Figure 10.—Superjacent strata conditions over 6, 7, and 8 development gate entry systems.

the strata movements and coal behavior associated with the bump phenomena.

### BUMP EVENTS IN 6 AND 7 DEVELOPMENT

The 6 and 7 development gate entry systems employed a 218-ft-wide yield-abutment-yield configuration with the yield pillars on 50-ft centers, the abutment pillars on 100-ft centers, and all crosscuts on 100-ft centers. This gate pillar configuration replaced an older yield-yield-abutment design, in which the same size pillars were employed; however, in the older design, the tailgate abutment pillar was located directly adjacent to the mined panel. In this previous design, the 80-ft-square pillars frequently experienced heavy bumps directly adjacent to the tail drive, causing coal to be thrown into the face area (5). However, in the yield-abutment-yield design, the 80- by 30-ft pillars reached their maximum load-bearing capacity and began to yield during the headgate pass of the face, thereby eliminating their potential to bump. The yielded pillars effectively shield workers from coal thrown in the event the 80- by 80-ft tailgate abutment pillar bumps during the subsequent tailgate pass.

Abutment pillar bumps began to occur adjacent to the tail drive within the 6 development gate entry system when 3,650 ft of panel S-6 had been mined. The bump area, labeled A in figure 10, was under 1,350 ft of overburden, 27 ft of sandy shale immediate roof, and 203 ft of quartzite main roof. Only slight movement of the face was observed on the tailgate end of the face line. Dramatic coal displacements were observed within the tailgate (fig. 11). No coal was disturbed in the headgate, in this or any of the bumps investigated during this study. The tailgate entry contained a double row of wooden cribs, spaced as displayed in figure 12. The fresh air intake entry, labeled as the smoke free, was supported by a double row of wooden posts, which allowed the area to be explored to the extent noted on figure 11.

Bump A was centered between pillars A and B on a line parallel with the longwall face. The smoke-free entry was completely closed by the rapid movement of the rib of abutment pillar A against yield pillar E. Similar abutment pillar rib movement closed the crosscuts between pillars A and B, and B and C. Yield pillars E through H were stationary, with only minor rib spalling as indicated on figure 11. Gaps between the siltstone immediate roof and the A and B abutment pillars ranging from approximately 2 to 12 in were formed by the bump. Roof-to-pillar gaps of this nature were evident over the bumped abutment pillars in the majority of the bumps discussed in this report. This reduction in roof-to-pillar contact area is dramatic

evidence of the minimal load carried by the abutment pillars immediately after the bump occurrence.

The shearer was cutting coal near the tail side of panel S-6 when bump A took place. None of the members of the face crew were injured; however, they reported experiencing the shock wave released by the bump. Ventilation devices located at the mouth of 6 development, over 2,000 ft away, were damaged.

Tailgate abutment pillar bumps, similar in magnitude to the 6 development event (bump A), occurred during the mining of panel S-7. However, abutment pillar bumping (bump B in figure 10) began approximately 450 ft earlier in panel mining. The B bump area was under 1,720 ft of overburden, 37 ft of sandy shale immediate roof, and 188 ft of quartzite main roof.

Given the same gate entry system design and the in-mine observations, the likelihood of bump occurrence is postulated to increase with increased overburden thickness, width of main gob (number of previous panels mined), extent of panel mined (length of gob resulting from active panel), and quartzite thickness. However, current theories suggest that a critical gob width is reached after the third panel in a series is mined. Thus, the bump potential may not increase significantly with increases in main gob width after the third panel is mined.

The fact that abutment pillar bumps of comparable magnitude did occur at sites A and B could be used to deduce the relative importance of each of the five main factors given above. The 7-pct decrease in quartzite main roof thickness and 37-pct increase in siltstone immediate roof thickness from site A to B did not reduce the bump potential. To the contrary, abutment pillar bumps were experienced 450 ft earlier in panel S-7 mining. Thus, these minor variations in roof rock layers may not be as important as the 27-pct increase in overburden thickness.

As the mining of panel S-7 progressed, the tailgate abutment pillars began progressively bumping 500 ft in advance of the longwall face. This violent failure of the tailgate abutment pillars transferred load to panel S-7, initiating the occurrence of bumps on the tailgate corner of the longwall panel. Two of the face bumps, labeled C and D on figure 10, were significant events that affected normal operations. The C and D bump events occurred after panel S-7 was mined to 4,240 and 4,430 ft, respectively, and occurred at the crosscut in the tailgate. A plan view of the C bump site is presented as figure 13. Both face bumps happened when the shearer was cutting from the head to the tail, in the area 20 to 40 ft from the tailgate corner of panel S-7. In bump D, the force of the bump lifted the panline and thrust it toward the gob. In both the C and D bumps, the rib of panel S-7 threw coal

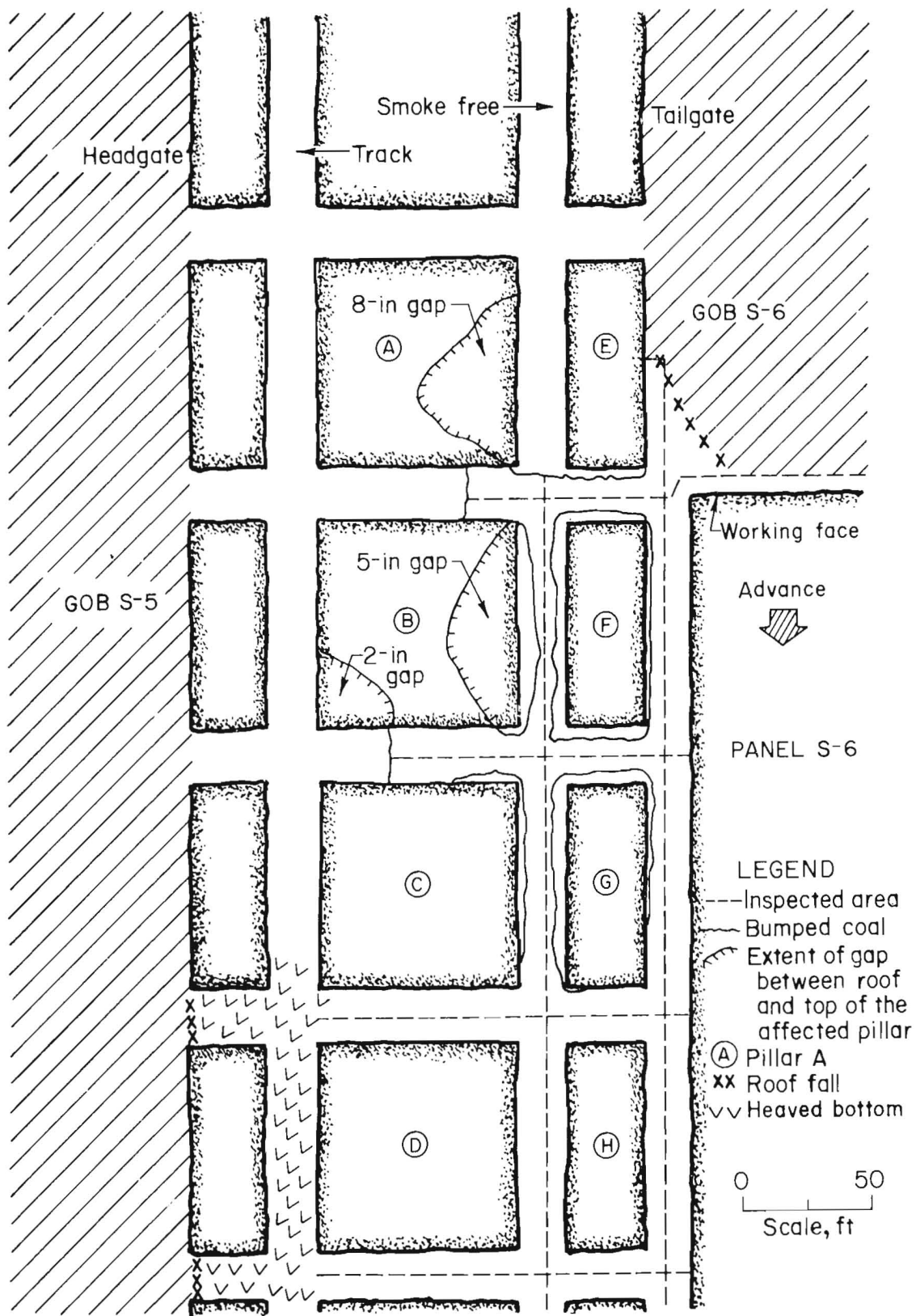


Figure 11.—Plan view of bump A (fig. 10) within 6 development gate entry system.



Figure 12.—Typical tailgate crib support configuration in 6 and 7 development gate entry systems.

into the tailgate entry for approximately 40 ft. Ventilation devices in the tailgate were not affected in either the C or D face bumps, indicating that abutment pillar bump events in the tailgate did not occur simultaneously with the face bumps.

A visual inspection of the pillar conditions in the tailgate after face bump C indicated that the load-bearing capacity of abutment pillars A through F was destroyed prior to the occurrence of face bump C (fig. 13). This failed condition is assumed for pillar C, as it could not be inspected. The entry between pillars B and I was completely closed by abutment pillar B's bumping, making travel down the smoke-free entry impossible. The area containing abutment pillars G, F, and E was inspected by approaching the C bump site from the submain. The entry between pillars D and K was not traveled. Figures 14A and 14B show the condition of the completely closed entry between abutment pillars E and F and the partially closed entry between abutment pillars F and G, respectively (fig. 13). In both entries, the posts were not broken by roof-to-floor convergence, which indicates the main overburden load was supported by panel S-7. Consequently,

the abutment pillars would not be expected to deform or punch into the bottom.

After the D bump, the tail of the face was kept 10 ft in advance of the head as much as possible. This procedure was implemented to decrease the stress concentration on the tail by redistributing stresses toward the head. It cannot be ascertained if the tail advancement procedure had the desired effect. Subsequent to the D bump, the shearer was operated remotely during panel S-7 mining. This procedure was a very positive step, as it allowed the longwall to advance to the completion of panel S-7 without further major face bump delays.

An abutment pillar bump (bump E in figure 10) similar to bumps at sites A and B was experienced after 4,860 ft of panel S-7 had been mined. Tailgate ventilation devices were affected. This bump is significant in that it marked the return to tailgate abutment pillar failure adjacent to or on the gob side of the longwall face. This reduction in the magnitude of the bump events may have been due to the now nearby barrier pillars, left to protect the submain entries from gob abutment loading.

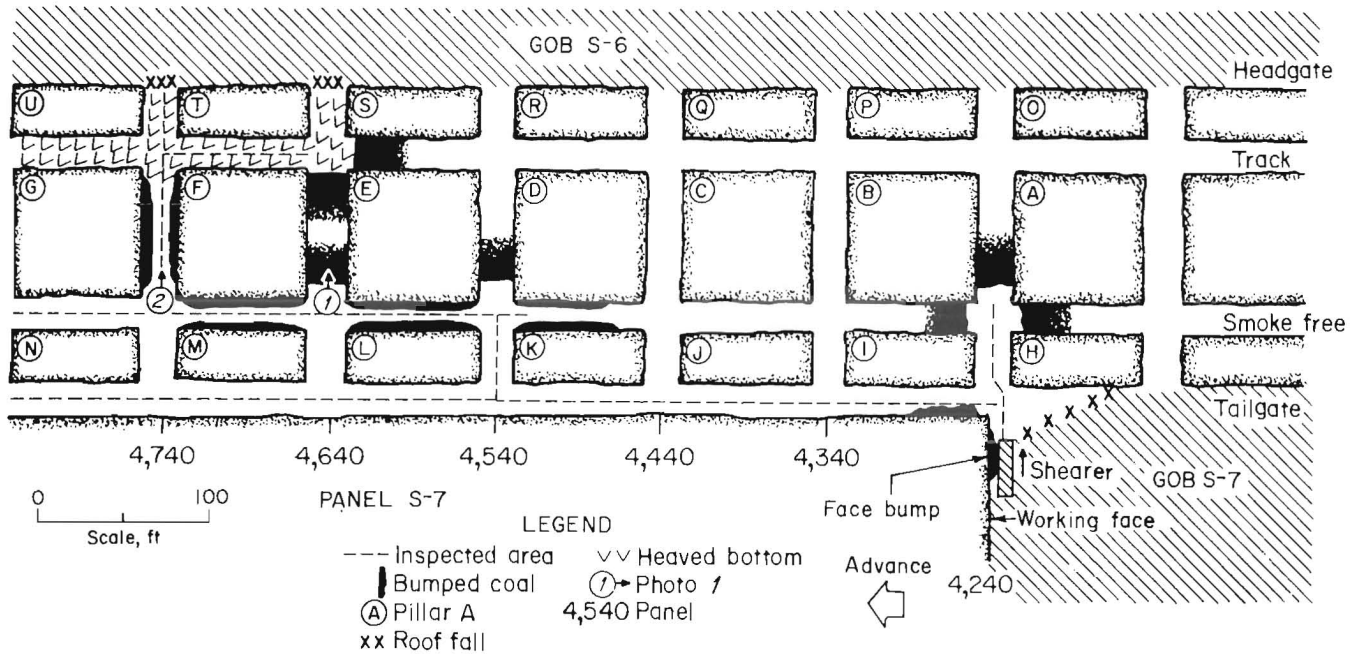


Figure 13.—Plan view of bump C (fig. 10) within 7 development gate entry system. Circled italic numbers denote locations from which photographs in figure 14 were taken.

### GROUND CONTROL EXPERIENCE IN 8 DEVELOPMENT

In an attempt to better control ventilation between previous and active gobbs, to improve tailgate entry stability, to control tailgate bumps, and to standardize gate entry system design, the mine modified the yield-abutment-yield configuration for the 8 development gate entry system. This new 238-ft-wide design consisted of yield pillars on 40-ft centers and abutment pillars on 140-ft centers. Between the yield pillars, the crosscuts were driven at 60° angles on 100-ft centers, whereas between the abutment pillars the crosscuts were driven at 90° angles on 200-ft centers. The new layout results in 20- by 80-ft yield pillars on either side of a 120- by 180-ft abutment pillar. The larger abutment pillars in this new design are intended to support the applied abutment loads and thus prevent the ground stresses from overriding the longwall face. Gauna (15) reports the new design requires less entry to be mined to advance the entire section, which generates an improvement through reduced mining requirements. However, leaving a larger pillar in the gob slightly decreases the extraction ratio. Continuous miner coal production rates were not negatively affected by the design change (15).

The 8 development would appear to be more bump prone than the 7 development, based on the factors that influence bump potential. The comparison of the geologic and mine geometry conditions at the 6 development A bump site and the 7 development B bump site pointed to the importance of overburden thickness as the major

factor determining bump proneness. This factor indicates that a more severe tailgate bump problem should have developed during the mining of panel S-8 than was experienced during the mining of panel S-7 (fig. 10). The quartzite thickness in the main roof is not a factor, since it is extremely consistent over the 6, 7, and 8 development gate entry systems. Siltstone immediate roof thickness is greatest over the 8 development gate entry system; however, a 37-pct increase in siltstone immediate roof thickness from bump site A to B apparently did not have the effect of reducing bump potential. Furthermore, a review of figures 8 and 9 reveals the immediate roof and floor within the 8 development gate entry system are made up of extremely competent rock types that can be classified as "bump prone."

The structural rigidity of the immediate roof and bottom within the 8 development gate entry system was confirmed by the conditions at site F (fig. 15). The length of active gob at site F is equivalent to that at bump site D in the 7 development gate entry system (fig. 10). Excellent roof and minimal bottom heave were encountered in the tailgate entry even with the face (fig. 16A). Spalling of panel S-8 rib into the tailgate entry was evident over approximately the first 40 ft in advance of the face. Minor instability was encountered during the mining of the face, in the area 20 to 40 ft from the panel S-8 tailgate corner (fig. 15). Coal cutting induced cracking and minor spalling of the face, indicating stress readjustment was taking place. While this minor face instability was slight compared with face bumps C and D, it is important to the subsequent analysis of pillar behavior under high stress. The tailgate



Figure 14.—Condition of (A) crosscut between pillars E and F (location 1, figure 13) and (B) crosscut between pillars F and G (location 2, figure 13).

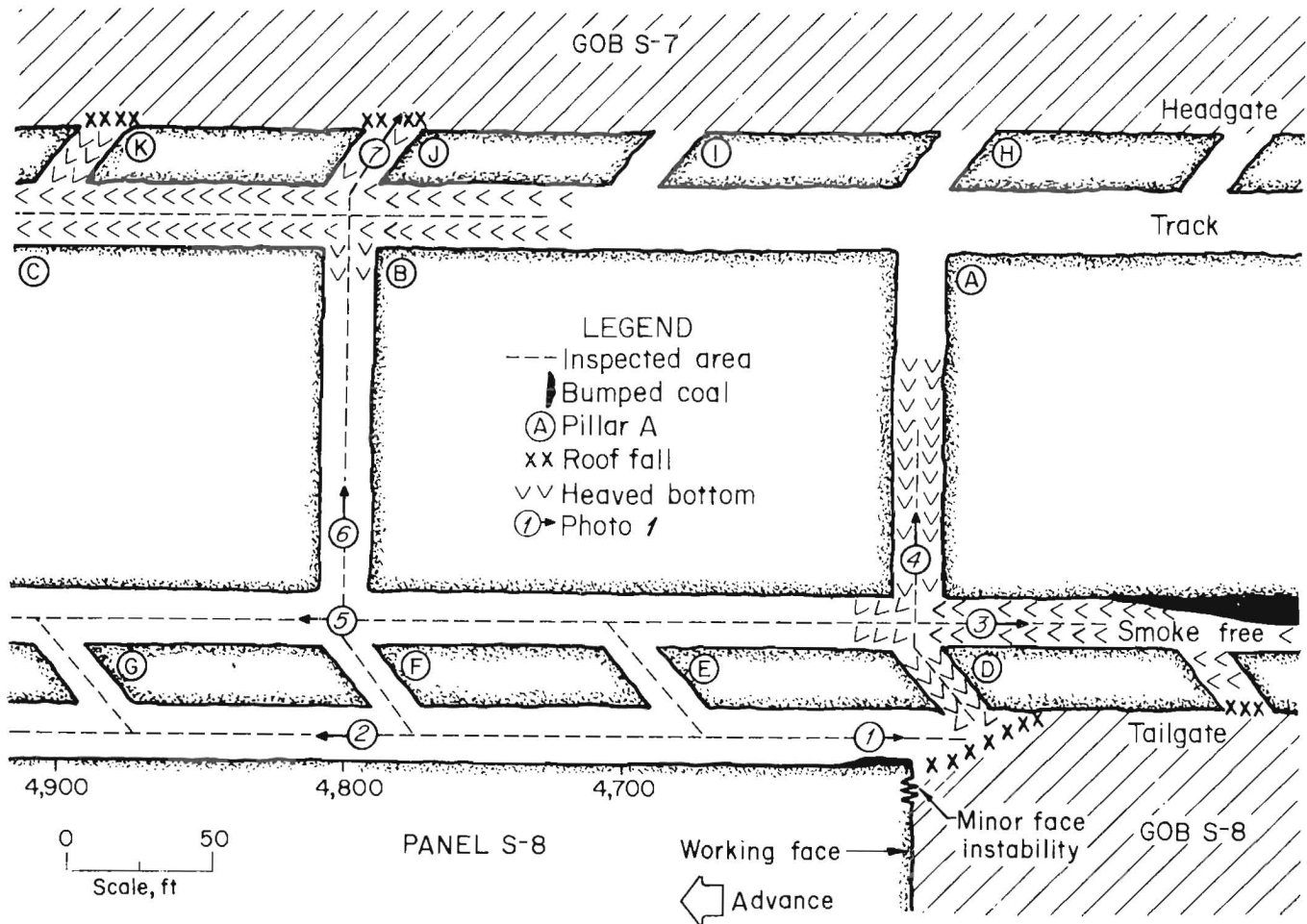


Figure 15.—Plan view of conditions at site F (fig. 10), within 8 development detailed study area. Circled italic numbers denote locations from which photographs in figure 16 were taken.

entry 200 ft in advance of the face was undisturbed by the mining of panel S-8 (fig. 16B).

Heaved bottom was found at or behind the face in the smoke-free entry (fig. 16C) and in the crosscut between abutment pillars A and B (fig. 16D). Bumping of abutment pillar A was noted approximately 100 ft behind the face (fig. 15). It appears that the 120- by 180-ft abutment pillars form a solid column that punches into the mine floor when they are subjected to high abutment zone stresses. However, the bottom appears to fail in a brittle fashion (fig. 16C). The smoke-free entry and the abutment pillar crosscut, 200 ft in advance of the face, were undisturbed by the mining of panel S-8. Figure 16E displays the excellent strata conditions, essentially unchanged since the completion of panel S-7, in the smoke-free entry between abutment pillar C and yield pillar G. The polyethylene pipe, suspended from the roof, contained the data acquisition cables. Continuous roof-to-floor convergence data, obtained by a data acquisition system, confirmed that abutment pillar bumping did not close the smoke-free entry up to 200 ft behind the face. Most of the crosscut between abutment pillars B and C, unchanged since the

completion of panel S-7, displayed minimal bottom heave (fig. 16F). However, the last 15 to 20 ft of the crosscut on the gob side experienced bottom heave, which resulted in approximately 15 in of roof-to-floor convergence, during the mining of panel S-7. Similar bottom heave behavior was also found in the track entry and the yield pillar crosscuts. The good roof conditions directly adjacent to the panel S-7 gob, at the crosscut between yield pillars K and J (fig. 16G), are representative of the entire study area.

The superior performance of the 8 development gate entry system design over the previous design was confirmed by in-mine observation. Under worst case conditions, the 120- by 180-ft abutment pillars did not begin to bump until they were approximately 100 ft behind the face. The previously employed 80-ft-square abutment pillars bumped 500 ft in advance of the face, allowing load transfer to the mined panel. Thus, the 180- by 120-ft abutment pillars within the 8 development gate entry system effectively shielded panel S-8 from the excess loads that resulted in the face bumps at the tailgate corner of panel S-7.

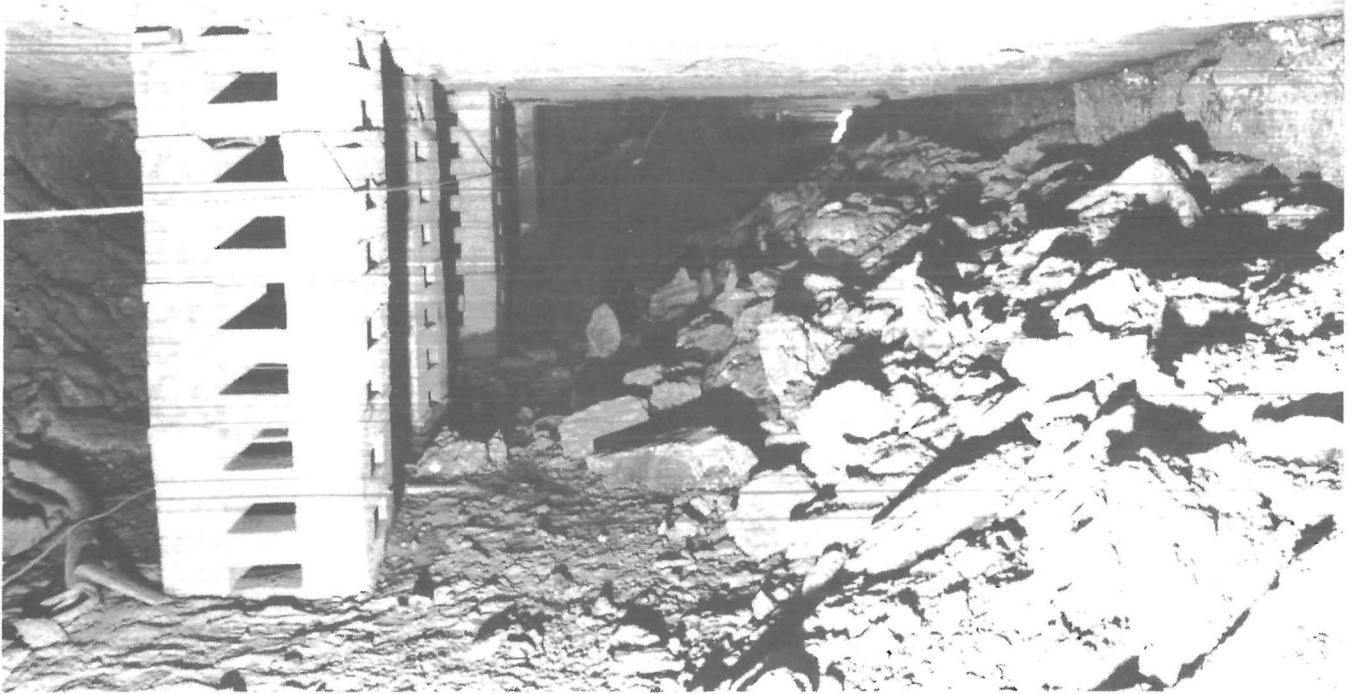
**A****B**

Figure 16.—Conditions within 8 development detailed study area. A, Good conditions at tail shield (location 1, figure 15); B, good tailgate entry conditions 200 ft in advance of mining panel S-8 (location 2, figure 15).



Figure 16.—Conditions within 8 development detailed study area—Con. C, Brittle failure of bottom in smoke-free entry adjacent to mining of panel S-8 (location 3, figure 15); D, conditions in abutment pillar crosscut adjacent to mining of panel S-8 (location 4, figure 15).

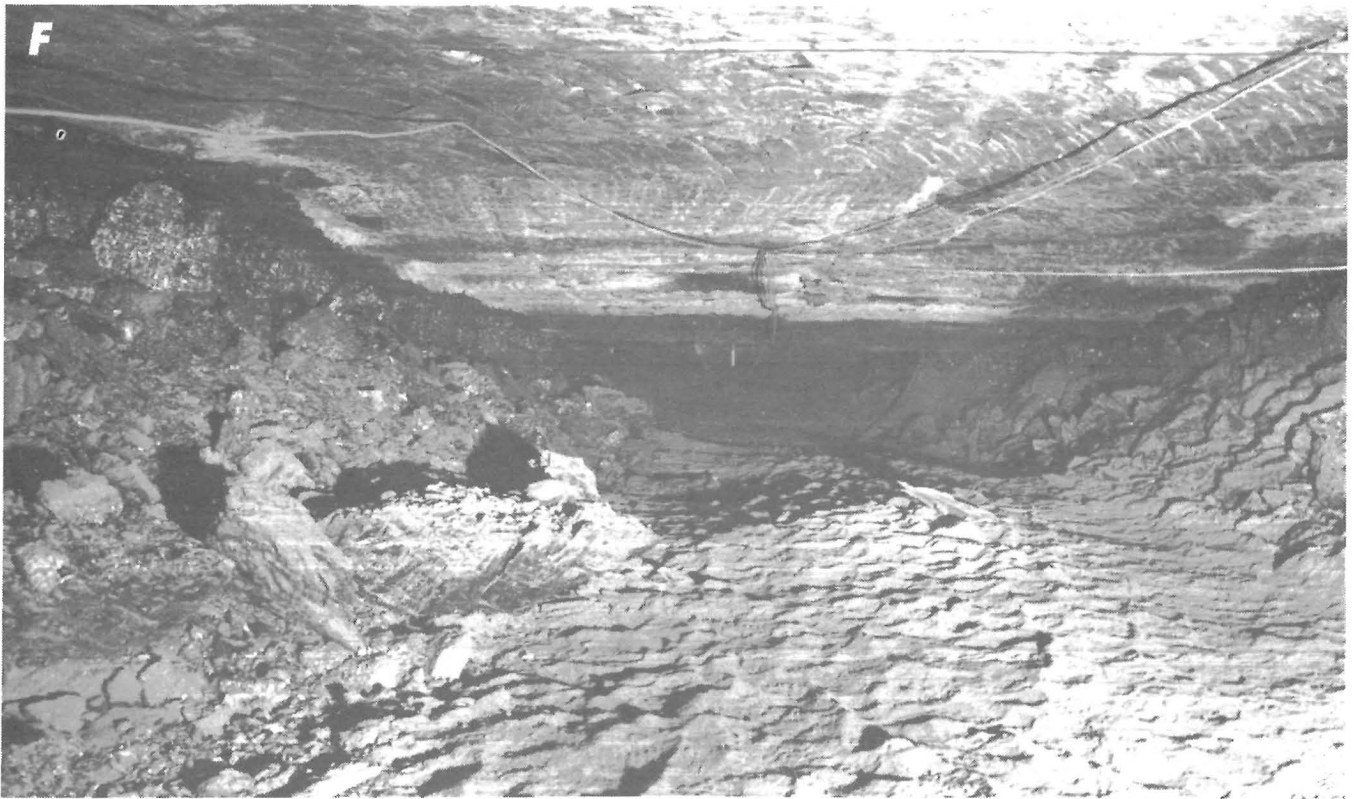


Figure 16.—Conditions within 8 development detailed study area—Con. *E*, Good strata conditions in smoke-free entry 200 ft in advance of mining panel S-8 (location 5, figure 15); *F*, good strata conditions in abutment pillar crosscut 200 ft in advance of mining panel S-8 (location 6, figure 15).

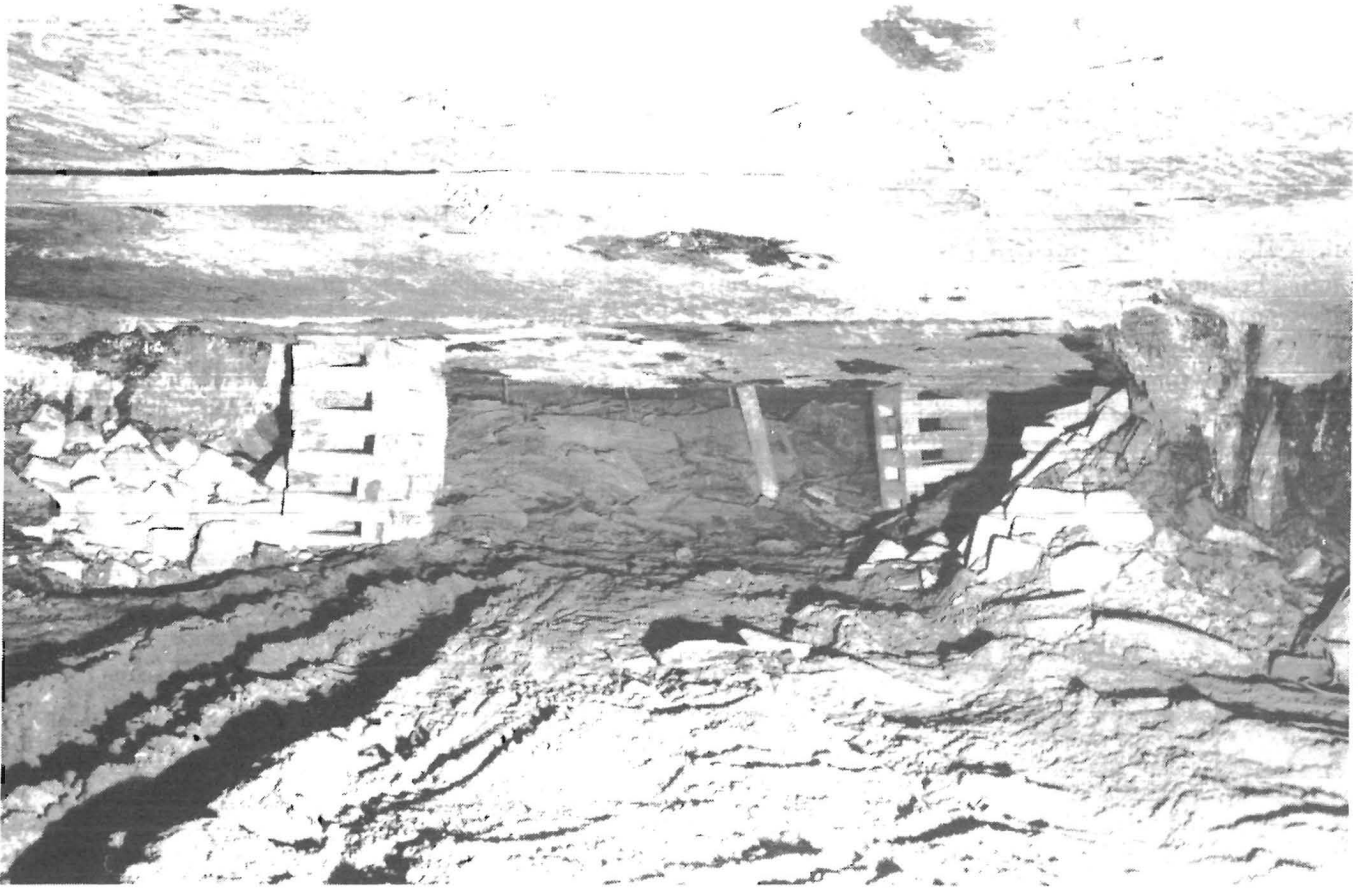


Figure 16.—Conditions within 8 development detailed study area—Con. G, Good strata conditions at edge of panel S-7 gob 200 ft in advance of mining panel S-8 (location 7, figure 15).

## QUANTITATIVE EVALUATION OF GATE ENTRY SYSTEM PERFORMANCE

The state-of-the-art instrumentation arrays utilized in the two detailed study areas consisted of 116 stainless steel borehole platened flatjacks (BPF's) for indicating changes in pillar stress, 8 coal extensometers for measuring pillar dilation, 133 convergence stations for measuring roof-to-floor closure, a differential roof-sag indicator for monitoring bedding separations in the roof, and a differential floor-heave indicator. The instrument configurations in the 7 and 8 development gate entry systems are shown in figures 17 and 18, respectively. Iannacchione (8), Heasley (16), and Campoli (17) have discussed this instrumentation and portions of the data collected. Each of the instrumentation schemes and their results will be discussed separately.

### BOREHOLE PLATENED FLATJACK

The Bureau designed, tested, calibrated, and manufactured the borehole platened flatjack (BPF) used in this study. The BPF is simple in design and rugged in construction (fig. 19). The installation of the BPF is simple and straightforward. Setting rods that allow horizontal and rotational control enabled the BPF units to be placed in 2-in-diameter boreholes that were drilled at midseam height (fig. 20). The conversion of the hydraulic pressure change in the BPF to actual in situ stress change is accomplished with a recently developed computer program called BPFICAL, developed by Heasley (18).

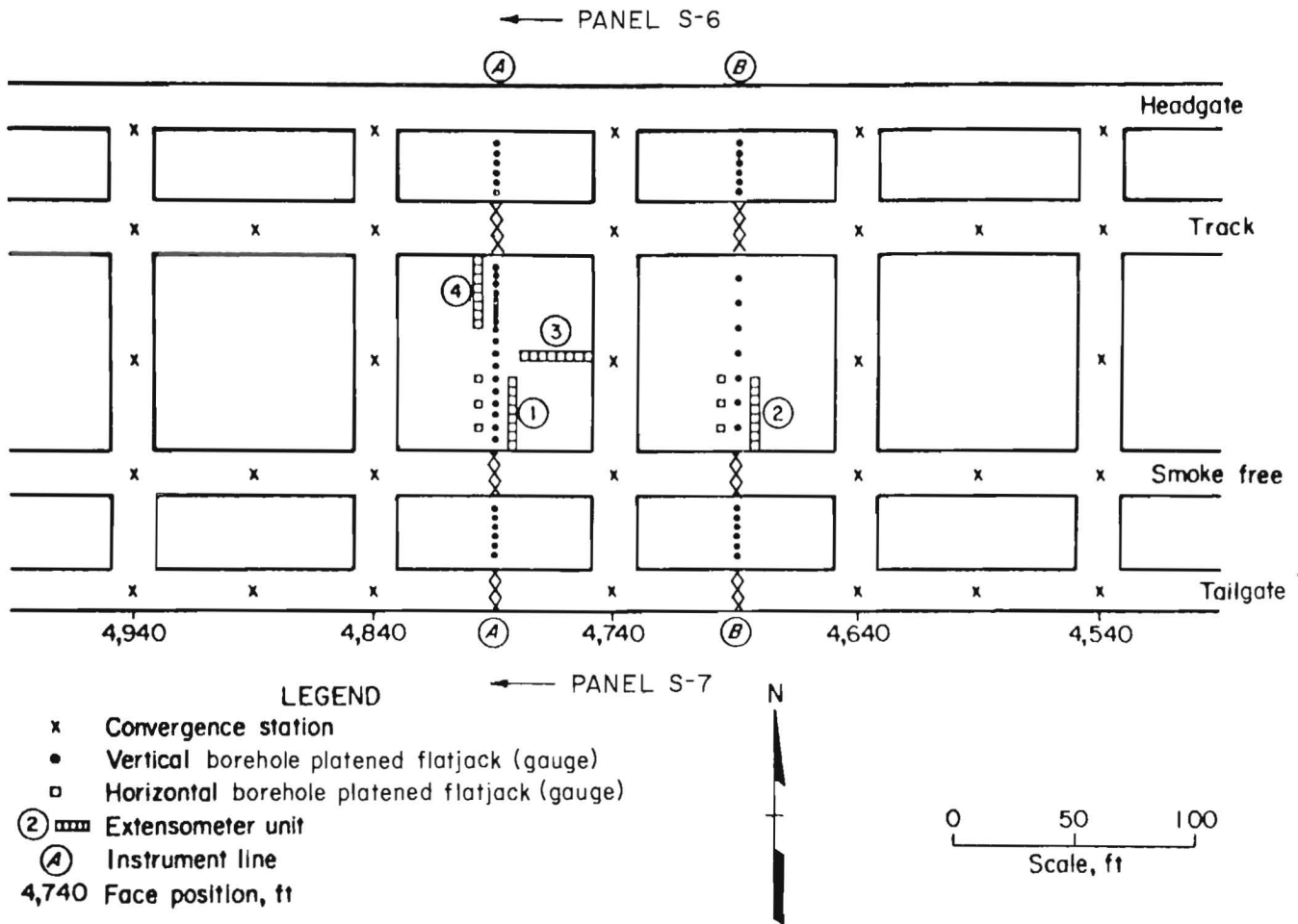


Figure 17.—Map of 7 development instrument array.

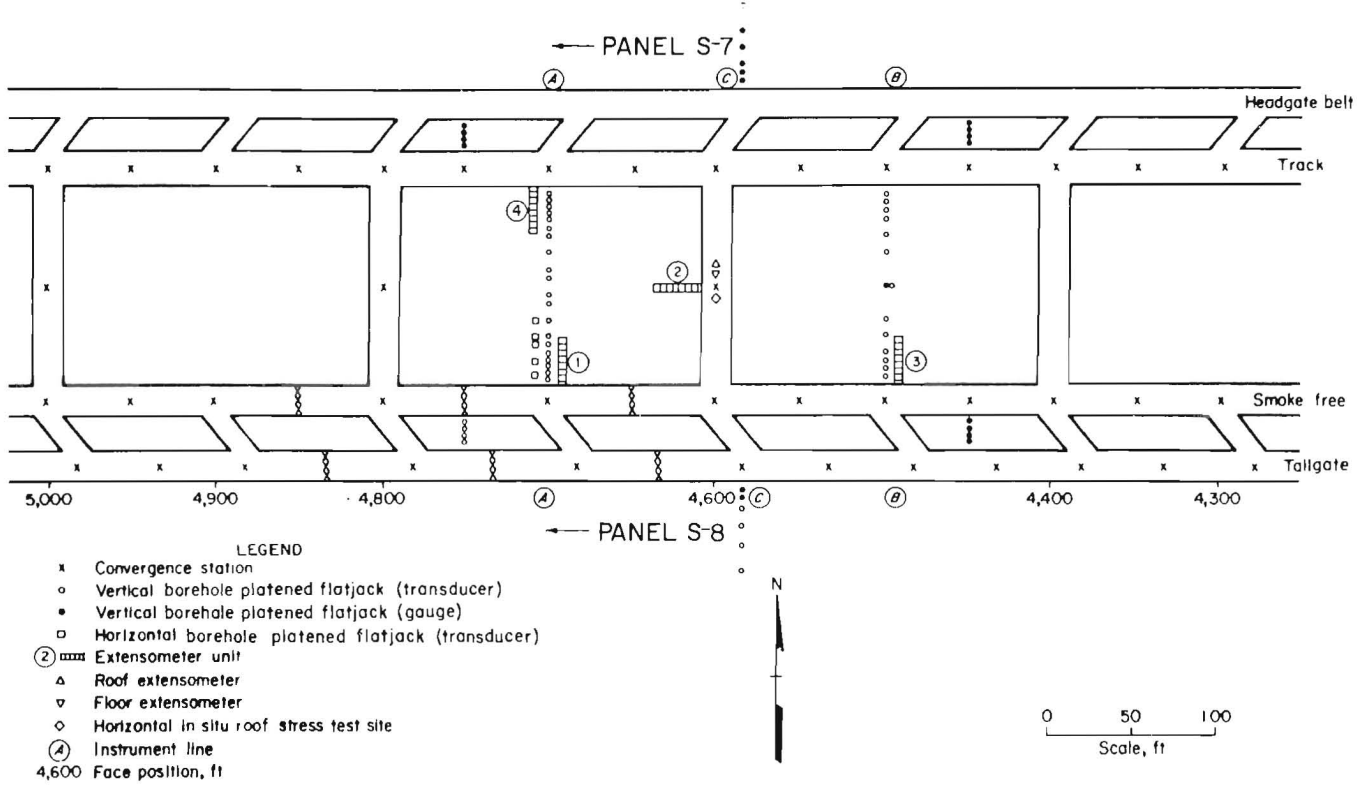


Figure 18.—Map of 8 development instrument array.

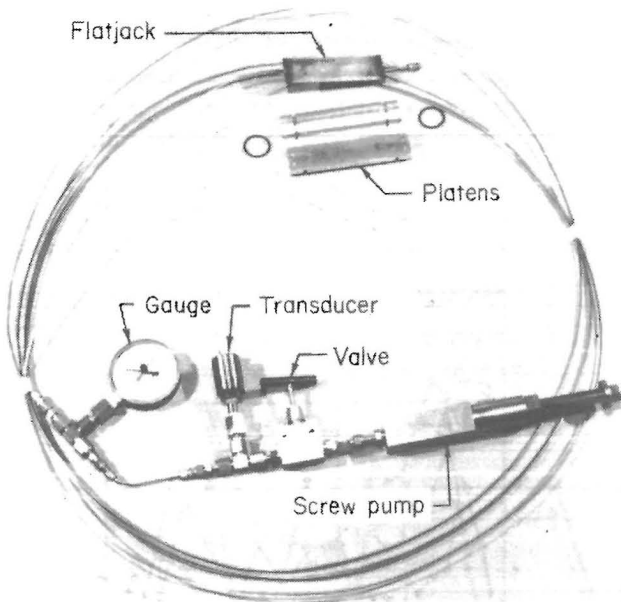


Figure 19.—Borehole platened flatjack configuration.



Figure 20.—Borehole platened flatjack installation procedure.

The main goal behind the BPF installation was to obtain pressure profiles across the width of the gate entry systems. Therefore, in contrast to the widespread installation of the convergence stations, the BPF's were installed in transverse lines across each gate entry system with each line bisecting the two yield pillars and an abutment pillar (figs. 17-18). A third line of BPF's was installed in panels S-7 and S-8 from the 8 development gate entry system (fig. 18). All of the BPF results described in this report pertain to pillar stress changes in the vertical direction.

After calibration by BPF<sub>CAL</sub>, the BPF data are postulated to be actual or very near actual in situ stress changes in the coalbed. Borehole irregularities and installation conditions are factors that may prevent an absolute pressure conversion; however, it is felt that the calibrated BPF data are at least very close to actual in situ stress changes in the coalbed. Only calibrated data are presented in this report and are hereafter referred to as "coalbed stress change." The coalbed stress change data were subjected to a linear interpolation by face position. This procedure allowed the coalbed stress change data for all BPF's to be plotted relative to rounded panel face position. Negative, zero, and positive relative face positions correspond to the face approaching, adjacent to, and past the instrument lines, respectively. Coalbed stress change data from the instrument lines within a given array are presented as if they were on a single line. These simplifying procedures are valid only because of the very consistent reaction of the coalbed, immediate roof, and immediate floor to the changing mine geometry.

### Coalbed Stress in 7 Development

#### Mining of Panel S-6

A definite asymmetrical reaction to the mining of panel S-6 is evident, with coalbed stress changes highest on the panel S-6 side of the 7 development gate entry system (fig. 21A). Minimal stress change was induced in the instrumented pillars until the mining of panel S-6 reached the -500-ft face position. When the face was adjacent to the instrument lines, a maximum coalbed stress change of approximately 8,500 psi was found in the head yield pillar. Mining at the 500-ft face position saw a dramatic drop in coalbed stress change within the head yield pillar, which is assumed to indicate the yielding of the section of the coalbed containing the BPF. At the same time, a maximum coalbed stress change of near 12,000 psi was measured on the headgate side of the 80-ft-wide abutment pillar.

The 30-ft-wide head yield pillar started to yield when the mining of panel S-6 was between 0 and 100 ft past the BPF array (fig. 21B). Only minor residual stresses

remained on the head yield pillar after the face was 300 ft past the instrument lines.

At least a 5-ft yield zone was generated in the outer perimeter of the 80-ft-wide abutment pillar when the mining of panel S-6 progressed 200 ft past the instrument array, shown by a drop in coalbed stress change at the BPF's positioned 5 ft into the pillar (fig. 21C). This drop in stress was partially due to the transfer of load from the head yield pillar. The yield zone in the abutment pillar enlarged to 15 ft into either side by the time the mining of panel S-6 was 500 ft past the instrument lines, reducing the width of the confined bearing area from 80 to 50 ft. At this time, maximum values of coalbed stress change occurred within the 32-ft-wide tail yield pillar (fig. 21A).

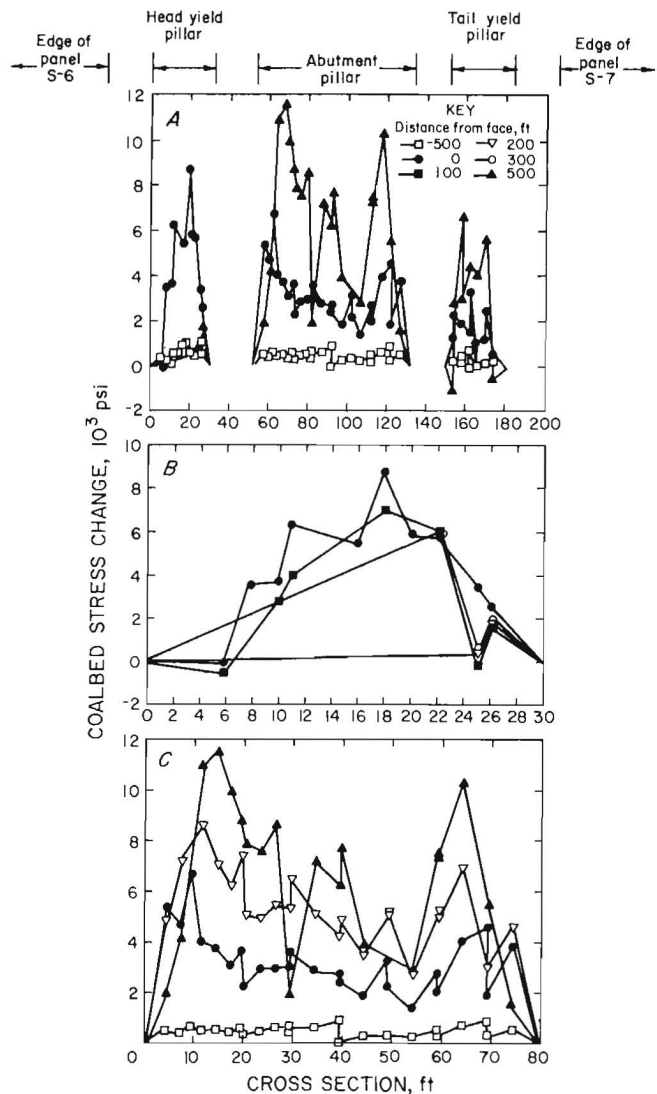


Figure 21.—Coalbed stress change in 7 development study area during mining of panel S-6. A, Across development cross section; B, across head yield pillars; C, across abutment pillars.

## Mining of Panel S-7

During the early mining of panel S-7 to the -3,000-ft distance from the instrument array, peak stress change remained virtually constant on the panel S-6 side of the abutment pillar, while stress in the pillar core and the panel S-7 side reduced significantly (figs. 21C-22). There are three points of view on why the drop in pillar core and the panel S-7 side stress was not accompanied by a drop in peak panel S-6 side stress. First, the drop in pillar stress over the panel S-7 side of the abutment pillar during this time period may be attributed to the simultaneous loss of support capacity in the tail yield pillars. Second, this trend may not be real, owing to the low number of operating BPF's; however, two horizontally oriented BPF's placed 10 and 30 ft into the panel S-7 side of the abutment pillar continued to measure significant horizontal confinement until the pillars began to burst at 500 ft in advance of the face. Third, Iannacchione (8) in an in-depth study of this situation stated, "Pillar failure occurred during a stable loading period and may be analogous to creep failure in laboratory test specimens."

Mining from the -3,000- to -1,100-ft distance from the instrument array did not affect the coalbed stress change profile across the 80-ft-wide abutment pillar (fig. 22). When the face moved from the -1,100- to the -1,000-ft position, the pressure in the five BPF's in the panel S-6 side of the abutment went to zero. This is presumed to be indicative of the failure of the gob side half of the abutment pillar. By the time the face was located at the -600-ft distance from the instruments, only one BPF remained active. This is presumed to be indicative of the failure of the panel S-7 side of the abutment pillar. It

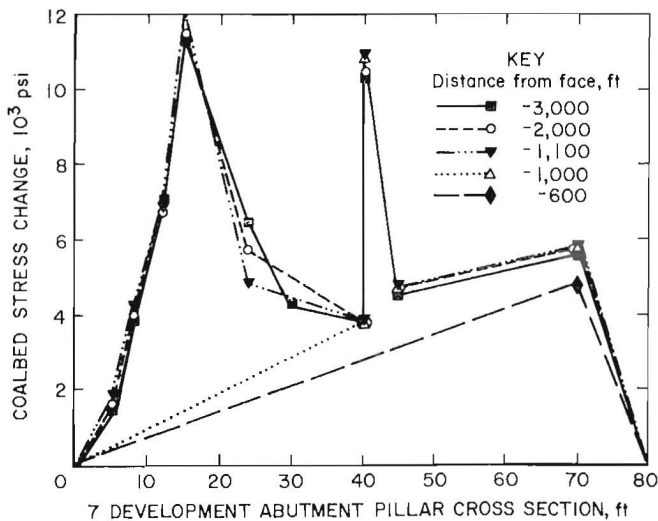


Figure 22.—Coalbed stress change across 7 development abutment pillars during mining of panel S-7.

would have been advantageous to have BPF's installed and monitored in the edge of panel S-7 to view load transfer from the gate pillars to the panel edge.

## Coalbed Stress in 8 Development

### Mining of Panel S-7

The instrumentation pattern employed in the 8 development gate entry system was very similar to the 7 development array, with the addition of the BPF's in the edges of panels S-7 and S-8 (fig. 18). The changes in coalbed stress for the 8 development gate entry system (fig. 23A), induced by the mining of panel S-7, display an asymmetrical pattern very similar to that of the stress changes in the 7 development gate entry system (fig. 21A).

The change in coalbed stress in the first 50 ft of the headgate edge of panel S-7, for eight selected face positions, is displayed in figure 24. The failure of the BPF located 50 ft into the panel edge is presumed to be due to instrument malfunction and not to mining geometry. Yielding of the coal 5 ft into the headgate edge of panel S-7 was initiated when the face was between 60 and 40 ft away from the instrument line. The yield zone never penetrated more than 10 ft into the panel edge during the mining of panel S-7. A maximum front abutment stress change of 6,000 psi was recorded immediately prior to the mining of the instrument. The change in coalbed stress more than 15 ft into the headgate edge of panel S-7 became more uniformly distributed as the face got closer to the instrument array. This can be seen from the near-zero slope of the change in stress curve between 15 and 35 ft into the panel edge, at the zero face position.

Only one BPF in the head yield pillars registered a stress change over 2,000 psi, at the 500-ft distance from the face position (fig. 23A). The BPF's in the head yield pillars were suspect from their installation, based on the coalbed's response to drilling and poor initial BPF response. From these two facts it is deduced that the head yield pillars had experienced too much deformation prior to instrument installation to provide true stress change results.

A 5-ft yield zone was generated in the outer perimeter of the 120-ft-wide abutment pillars when the mining of panel S-7 was between 0 and 200 ft beyond the instrument lines (fig. 23B). This can be seen by observing the decrease in coalbed stress change 5 ft into either side of the abutment pillars when the face was between 0 and 200 ft beyond the instrument lines. The yield zone enlarged to 10 ft into either side of the abutment pillars when the mining of panel S-7 was 500 ft beyond the instrument lines. Thus, the width of the stable bearing area for the abutment pillar was reduced from 120 to 100 ft by the time the face was 500 ft beyond the instrument lines,

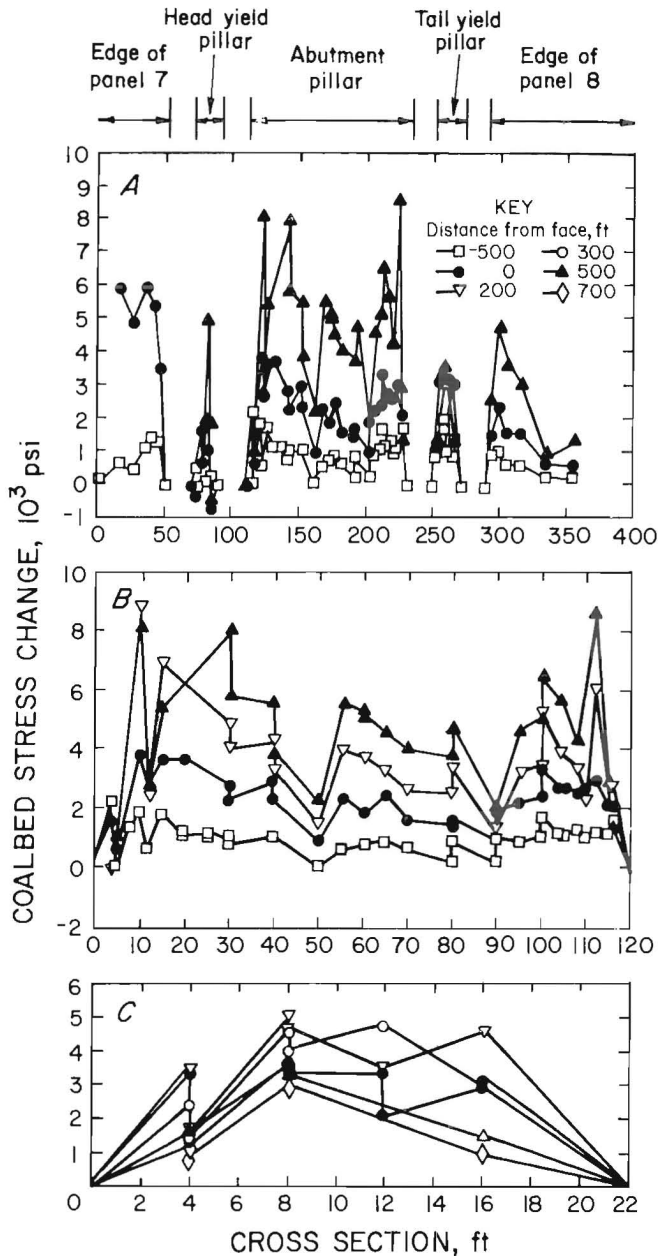


Figure 23.—Coalbed stress change in 8 development study area during mining of panel S-7. A, Across development cross section; B, across abutment pillars; C, across tail yield pillars.

compared with 50 ft for the 7 development pillar. A comparison of the two curves showing a 500-ft distance from the face reveals that the average stress change was approximately 2,000 psi lower across the 8 development abutment pillars (fig. 23B) than across the 7 development abutment pillars (fig. 21C).

The 22-ft-wide tail yield pillars in 8 development gate entry system began to fail when the mining of panel S-7 was between 200 and 300 ft beyond the instrument lines (fig. 23C). This is in contrast to the 32-ft-wide tail yield

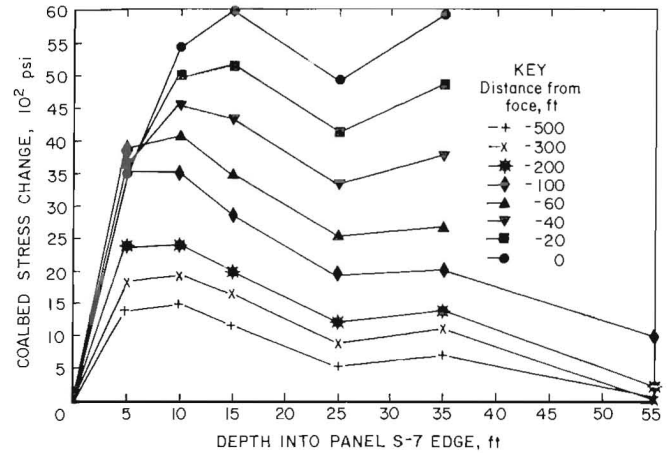


Figure 24.—Coalbed stress change across edge of panel S-7 during mining of panel S-7.

pillars in 7 development, which did not fail until the 500-ft distance from the headgate pass. Therefore, it is assumed that the earlier failure of the head yield pillars in 8 development is due to the 10-ft reduction in pillar width. The wider 7 development tail yield pillars (fig. 21A) displayed roughly twice the stress change of the 22-ft-wide tail yield pillars in 8 development (fig. 23C), at the 500-ft distance from the face position.

The first 65 ft of the tailgate edge of panel S-8 was instrumented with six BPF's (fig. 25). The coal 5 ft into the edge of panel S-8 began to yield when the mining of panel S-7 was between 300 and 400 ft past the instrument line, as demonstrated by its inability to take on additional load after this time. The formation of this 5-ft-wide perimeter occurred slightly after the tail yield pillars reached their ultimate strength. The 10-ft depth into the tailgate edge of panel S-8 was the consistent location of the maximum side abutment pressure, after the mining of panel S-7 passed the instrument line (fig. 25). Beyond the 10-ft perimeter, the coalbed stress change lessened with increased depth. However, the 65-ft depth still experienced a near 2,000-psi stress change, indicating that the mining of panel S-7 affected at least that depth of panel S-8.

### Mining of Panel S-8

Mining of panel S-8 did not significantly affect the coalbed stress profile across the 120-ft-wide abutment pillars until the face came within -200 ft of the instrument lines (fig. 26). At that point the panel S-7 side of the abutment pillar is presumed to have failed. This caused a significant increase in stress change in the panel S-8 side, with a maximum stress change of 12,000 psi occurring 17 ft into the panel S-8 side of the abutment pillar. Thus, only the 70-ft zone from approximately 35 to 105 ft from the panel S-7 side of the abutment pillar was providing significant load

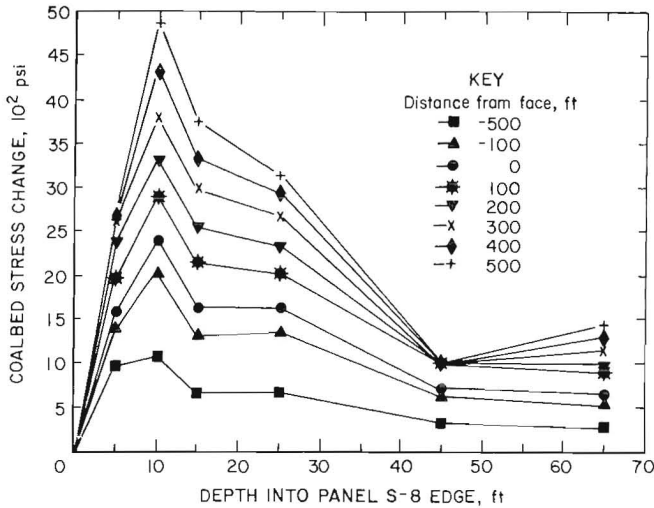


Figure 25.—Coalbed stress change across edge of panel S-8 during mining of panel S-7.

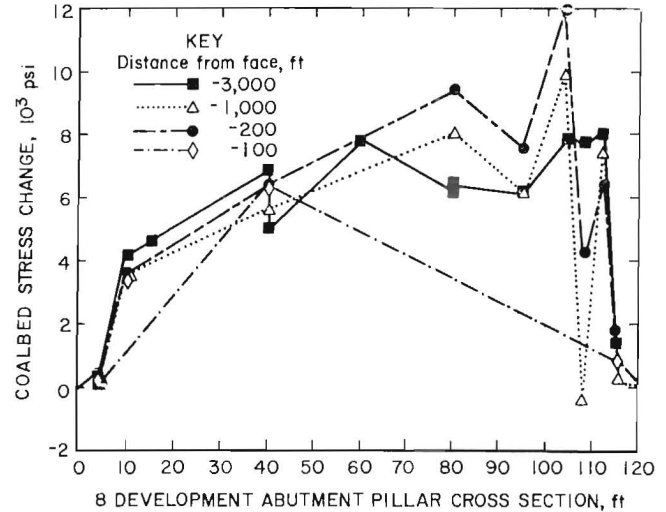


Figure 26.—Coalbed stress change across 8 development abutment pillars during mining of panel S-8.

resistance (fig. 26). Only one BPF displayed a significant change in stress at the -100-ft face position, indicating the failure of the panel S-8 side of the abutment pillar. As mentioned, similar behavior was experienced at the -600-ft face position in the 7 development gate road (fig. 22). No BPF's were functioning in either of the 120-ft-wide abutment pillars when the face was adjacent to the instrument lines.

The coalbed stress change in panel S-8 was measured over only the first 45 ft of the tailgate edge (fig. 27). The BPF located 65 ft into the panel edge (fig. 25) failed under long-term load, prior to near mining of panel S-8. The yielded perimeter increased from 5 ft to approximately 15 ft at the -500-ft distance from the face position. This can be seen by the decrease in the stress change from approximately 7,000 psi to less than 1,000 psi at a 10-ft depth into the panel, from the -1,000- to -500-ft distance from the face position. The 15-ft depth into panel S-8 was subjected to the maximum front abutment stress (11,500 psi) just prior to instrument extraction. The stress change recorded at the 25-ft depth when the face was nearly adjacent to the instrument line was almost identical to the pressure of the 15-ft mark, signifying that the front abutment pressure became more uniform across the longwall panel as the face approached the instruments. As discussed in the qualitative analysis section, face instability was evident 20 to 40 ft from the tailgate edge of panel S-8 (fig. 15). Thus, it is postulated that the longwall face ultimate strength for these geologic conditions is equal to or greater than 12,000 psi over the development stress.

### Average Weighted Coalbed Stress

The coalbed stress change analysis demonstrates the increased resistance to load provided by the 8 development gate entry system, as opposed to the 7 development configuration. This point is further reinforced by a weighted-average evaluation of pillar stress change. An average weighted coalbed stress change was calculated for each of the yield and abutment pillars in the studied gate entry systems, so their behavior during headgate and tailgate panel mining could be better understood and analyzed. This average weighted stress change for the various distances from the face position was computed by determining the sum of the incremental areas under the stress change curve for each pillar and then dividing the sum by the width of the pillar.

A direct comparison of the 7 and 8 development head yield pillar designs during headgate panel mining is clouded by the suspect behavior of the BPF's in the 20-ft-wide head yield pillars in the 8 development. Thus, the head yield pillar plot of average weighted stress change for the 8 development contained in figure 28A is possibly the actual postfailure behavior. The 30-ft-wide head yield pillars in the 7 development sustained a maximum average stress change of approximately 3,600 psi prior to failure. Weighted average stress change calculations indicate that failure occurred with the arrival of the headgate face on the instrument lines.

The tail yield pillars in both the 7 and 8 development gate entry systems obtained their average weighted

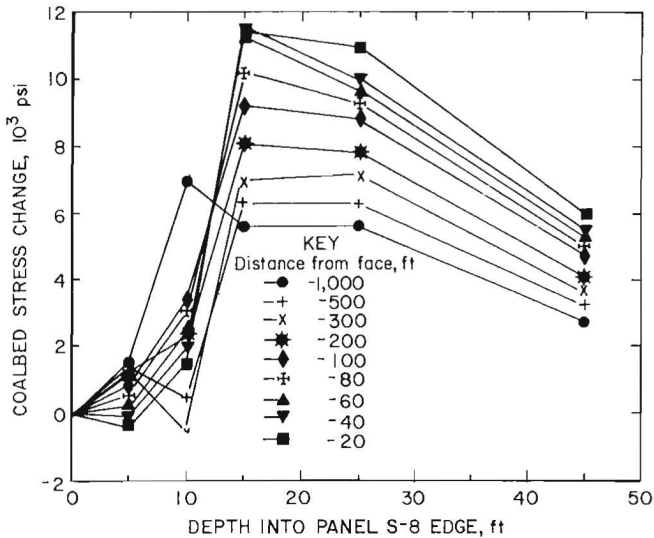


Figure 27.—Coalbed stress change across edge of panel S-8 during mining of panel S-8.

ultimate strength and started to fail during headgate panel mining (fig. 28B). The 32-ft-wide tail yield pillar in 7 development reached its average weighted ultimate strength of 2,500 psi at the 500-ft distance from the face position. In contrast, the 22-ft-wide tail yield pillar in 8 development reached its average weighted ultimate strength of 3,000 psi at the 200-ft distance from the face position.

Before the face reached the -100-ft position, the 120-ft headgate abutment pillars achieved a slightly higher average weighted stress change than did the 80-ft headgate abutment pillars for a given face position (fig. 29A). This minor difference (500 psi) is due to either the earlier installation of the BPF's or the reduced width of the head and tail yield pillars in the 8 development instrument array. When the mining of the panel was at or beyond the instrument lines, the 80-ft headgate abutment pillars were subjected to higher average stress change levels than the 120-ft headgate abutment pillars for a given face position. The average weighted change in headgate abutment pillar stress at the completion of panel mining was approximately 5,800 and 5,400 psi for the 7 and 8 development designs, respectively. The average weighted change in the 7 development tailgate abutment pillar stress gradually dropped from 5,800 to 4,300 psi during the mining of the first 1,500 ft of the panel (fig. 29B). As was previously discussed, this is attributed to the failure of the panel S-7 side BPF's or creep failure under near-ultimate strength. Subsequently, the average weighted tailgate abutment stress change stabilized at approximately 4,300 psi, until structural failure of the 80-ft-wide tailgate abutment pillars occurred at 1,000 ft in advance of mining. In contrast, the 120-ft-wide tailgate abutment pillars maintained an average

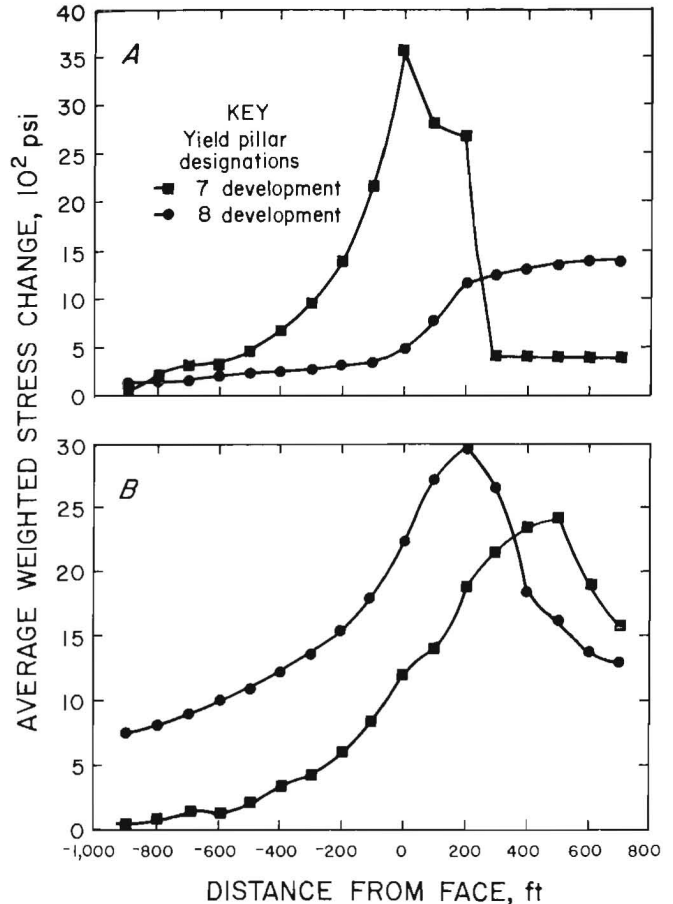


Figure 28.—Average weighted coalbed stress change in head (A) and tail (B) yield pillars during headgate panel mining.

weighted stress change of approximately 5,500 psi, until structural failure occurred at 5,800 psi at 200 ft in advance of mining. Therefore, the results from the BPF instrumentation showed the 120- by 180-ft abutment pillars in 8 development were much more stable than the 80-ft-square abutment pillars in 7 development.

#### ABUTMENT PILLAR DILATION

Multipoint extensometers were employed to investigate the edge behavior of highly stressed coal pillars, in an attempt to further define the depth of the yielded perimeter that confines the highly stressed core. Coalbed stress change results located this perimeter zone at approximately 15 ft into the abutment pillar edge. Four wire extensometers were grouted into midseam-height, horizontal drill holes in each of the 7 and 8 development instrument arrays. The units were oriented to measure pillar dilation parallel and perpendicular to BPF instrumentation lines (figs. 17-18). Each extensometer consisted of 10 anchors positioned within the first 30 ft of the

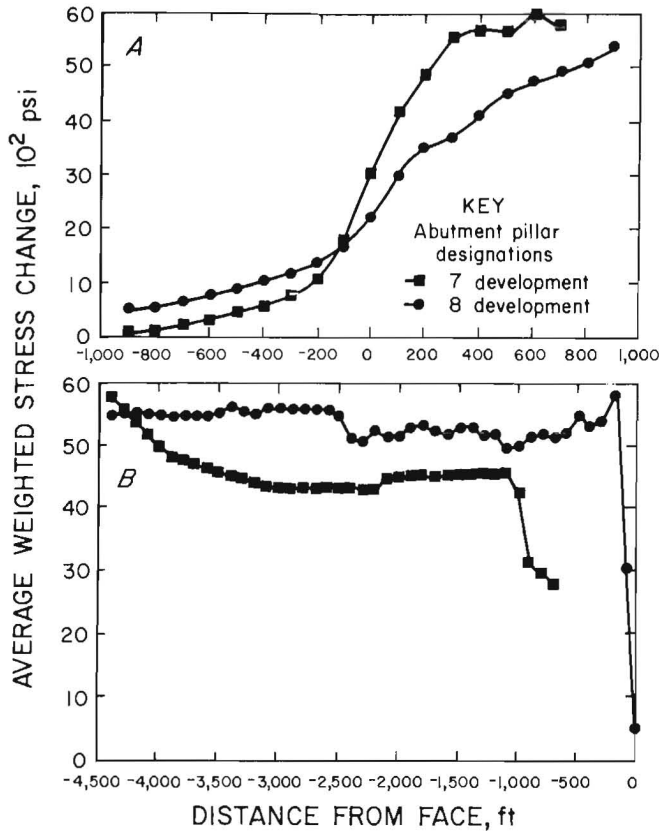


Figure 29.—Average weighted coalbed stress change in abutment pillars during headgate (A) and tailgate (B) panel mining.

abutment pillar edge. The anchors of each extensometer array were positioned at 4-, 8-, 10-, 12-, 14-, 16-, 18-, 20-, 25-, and 30-ft distances from the outer edge of the abutment pillars. All units were handread during headgate and tailgate passes. Thus, safety considerations controlled the frequency and termination of data collection.

The coal pillar dilation data were subjected to a linear interpolation by face position, just as the coalbed stress change data had been. Again, this procedure allows for analysis at rounded distances from the face positions. Thus, the necessity of matching the face positions exactly was circumvented. These two steps allowed the coal pillar edge dilation measurements to be viewed as if the data were continuous. Again, these simplifying procedures are valid only because of the consistent reaction of the coalbed, immediate roof, and immediate floor to the changing mine geometry. All of the dilation data are presented as strain (inch per inch) in a graphic format. Strain values are plotted at the midpoint of the interval between anchors. For example, an increase of 6 in. in the distance between the extensometer head and the 4-ft-deep anchor is represented as 0.125 in/in strain at a 2-ft depth into the pillar.

Figures 30A and 30B graphically display the strain recorded across the four extensometers located within the

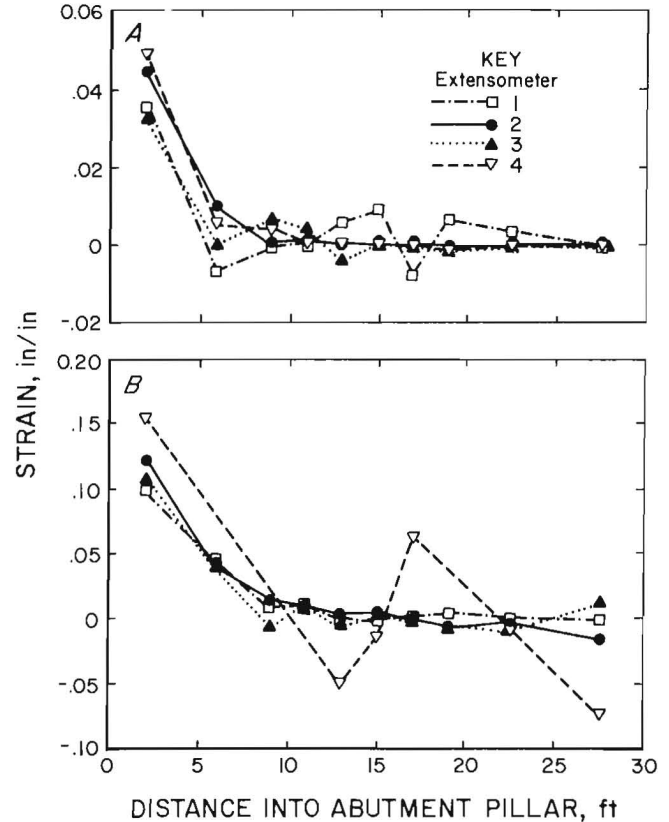


Figure 30.—Strain in perimeter of 7 development abutment pillars during mining of panel S-6. (A), Zero face position; (B) 500-ft face position.

7 development instrument array when the mining of panel S-6 was adjacent to and 500 ft outby the extensometers, respectively. When the mining of panel S-6 was adjacent to the units, the maximum strain value was recorded over the first 4 ft of the abutment pillar edges, with significant strain occurring up to 10 ft into the pillars (fig. 30A). The dilation of the 80-ft-square abutment pillars does not seem to be sensitive to extensometer orientation, indicating the pillar is uniformly deforming under the load. Peak changes in pillar stress of approximately 6,000 psi were measured at approximately 10 ft into either side of the abutment pillar, at the zero face position (fig. 21C). When mining of panel S-6 was 500 ft past the extensometers, 5 of 10 anchor points within extensometer 4 malfunctioned, and 2 of the deeper remaining anchors reported exaggerated strains (fig. 30B). However, the remaining three extensometers displayed a disturbed zone 15 ft around the 80-ft-square pillar's perimeter. This closely correlates with the change in pillar stress data reported for the 500-ft distance from the face position (fig. 21C).

The mining of panel S-7 from the -3,000- to -1,000-ft distance from the extensometers did not induce additional strain in the abutment pillar edges (fig. 31). This substantiates the lack of coalbed stress change reported for

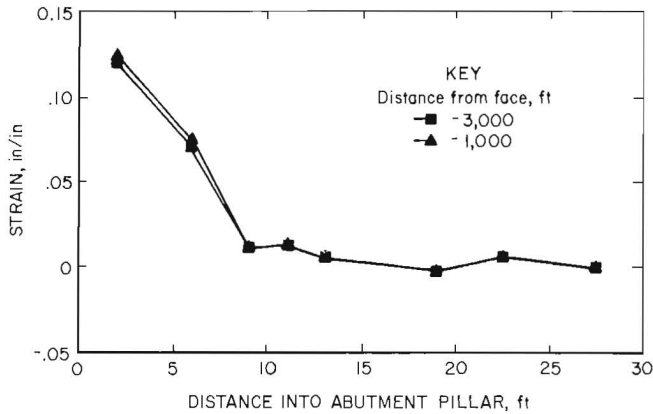


Figure 31.—Strain recorded in extensometer 1 in 7 development abutment pillar during panel S-7 mining.

the same time period (fig. 22). The danger of abutment pillar bumps in the 7 development gate entry system directly in advance of panel S-7 mining precluded subsequent data collection.

Figures 32A and 32B graphically display the strain recorded across the four extensometers located within the 8 development instrument array when the mining of panel S-7 was adjacent to and 500 ft outby the extensometers, respectively. When the mining of panel S-7 was adjacent to the units, the maximum strain value was recorded over the first 4 ft of the abutment pillar edge, with significant strain occurring up to 8 ft into the pillars (fig. 32A). The dilation of the 120- by 180-ft abutment pillars appears to be more pronounced on the panel S-7 side, as demonstrated by extensometer 4, when at the zero face position (fig. 32A). Peak changes in pillar stress of approximately 4,000 psi were measured at approximately 8 ft into either side of the abutment pillar, at the zero face position (fig. 23B). When mining of panel S-7 was 500 ft past the extensometers, extensometer 4 was not read because of safety considerations (fig. 32B). However, the remaining three extensometers displayed a disturbed zone of approximately 10 ft in the 120- by 180-ft abutment pillar's perimeter (fig. 32B). This closely correlates with the change in pillar stress data reported for the 500-ft distance from the face position (fig. 23B).

As was the case for the 80-ft-square abutment pillars, the mining from the -3,000- to -1,000-ft distance from the extensometers did not induce additional strain in the 120- by 180-ft barrier pillar edges. This is confirmed by extensometer 1's behavior at the -1,000-ft distance from the face position (fig. 33). As mentioned, coalbed stress change data also displayed minimal far-mining effect on the 120- by 180-ft abutment pillars in 8 development (fig. 26). However, both data sets indicate that the abutment pillars were affected by mining at the -200-ft distance.

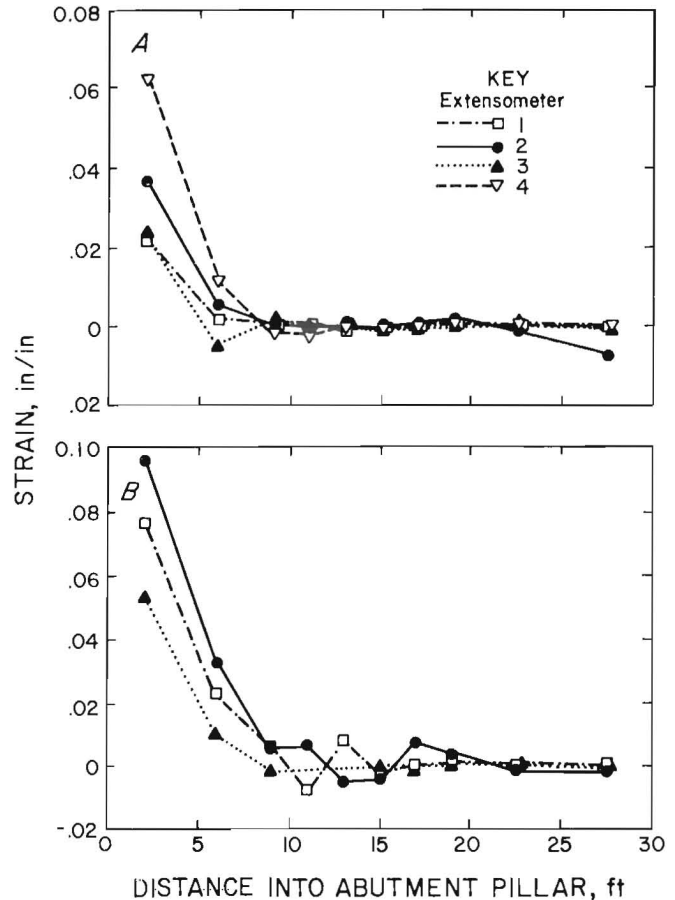


Figure 32.—Strain in perimeter of 8 development abutment pillars during mining of panel S-7. (A), Zero face position; (B) 500-ft face position.

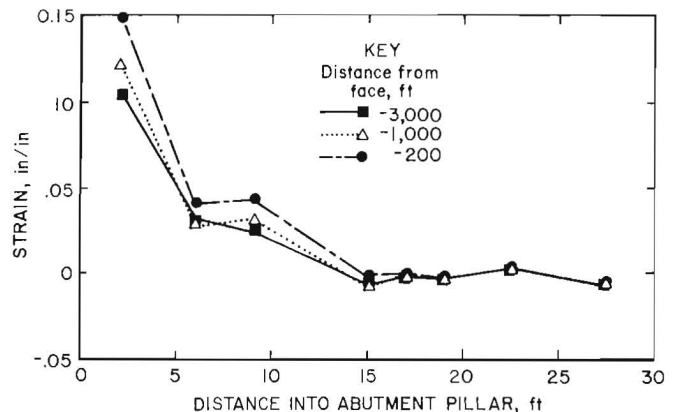


Figure 33.—Strain recorded in extensometer 1 in 8 development abutment pillar during panel S-8 mining.

The analysis of the coal extensometers installed in the abutment pillars in the 7 and 8 development gate entry systems demonstrated that both abutment pillar sizes formed a 12- to 15-ft-wide yielded perimeter zone. The

earlier reported coalbed stress change data place the depth of the yield zone at 15 ft. The width of the yield zone in Pocahontas No. 3 Coalbed pillars at near-ultimate stress is concluded to be 15 ft, and that width does not significantly change when the two-dimensional size is increased. However, dramatic changes in coalbed thickness could alter the depth of the yield zone. Therefore, any increase in pillar size results in a direct increase in confined core size at ultimate strength. Based on the 15-ft-wide yield zone, the ratio of core area to original pillar area for the 80-ft-square and 120- by 180-ft abutment pillars is 0.39 and 0.63, respectively. Thus, both the BPF and coal extensometer instrumentation point to the increased area of confined core as the explanation of superior performance of the 8 development design over the 7 development design for controlling tailgate abutment pillar bumps and their resulting longwall face bumps.

## MINING-INDUCED ROOF AND FLOOR DEFORMATION

### Roof-to-Floor Convergence

In general, the convergence stations were installed in all of the nearby intersections and at the midpoints of the instrumented abutment pillars in order to provide an overall view of the entry closure in the study areas. However, at certain locations, coinciding with the lines of BPF's, five convergence stations were installed in a line across the entry to obtain a profile of the relative roof-to-floor closure (figs. 17-18). The convergence stations consisted of permanent pins installed in the roof and floor, and a portable, telescoping rod that can measure the distance between the permanent pins to within several thousandths of an inch (fig. 34). The data acquisition system was used to remotely monitor roof-to-floor convergence. The sensor employed was a string pot potentiometer, capable of measuring up to 10 in of closure (fig. 35). It should be noted that it is not possible to directly distinguish between associated strata separation and pillar strain with this methodology; therefore, only the relative closures between the roof and floor are reported.

Once normalized for face position, the roof-to-floor convergence data were subjected to a linear interpolation by face position, just as the coalbed stress change and coal pillar dilation data had been. These two steps allowed the roof-to-floor convergence to be viewed as if all the stations within a given gate entry system were on a single line from one panel edge to another. The remarkably similar behavior of convergence stations located within the 450-ft-long 7 development array and within the 725-ft-long 8 development array confirm the very consistent reaction of the coalbed, immediate roof, and immediate floor to the changing mine geometry.

The roof-to-floor convergence was uniform and minor across the 7 development gate entry system until the mining of panel S-6 was adjacent to the instrumentation (fig. 36A). At this 0-ft face position an entry closure of approximately 1 in surrounded the head yield pillar, which was at its ultimate stress (fig. 21A). When the distance from the face position reached 500 ft, the head yield pillar had failed (fig. 21A); this coincided with roof-to-floor convergence of over 4 in. in its surrounding entries (fig. 36A). In-mine observations and convergence readings confirm the 80-ft-square abutment pillar allowed the roof to tilt toward the panel S-6 gob. This is reflected at the 500-ft distance from the face position by both the coalbed stress change data (fig. 21A) and the roof-to-floor convergence data (fig. 36A).

Entry closure continued during the mining of panel S-7; however, the slope of the tilt toward panel S-6 gob did not change (fig. 36B). This lends support to the creep failure mechanism proposed by Iannacchione (8) or the pillar core punching response. At the -600-ft distance from the face position, just prior to the beginning of the 80-ft-square tailgate abutment pillar bumps, the roof-to-floor



Figure 34.—Roof-to-floor convergence measurement with portable, telescoping rod.



Figure 35.—String pot potentiometer, remote reading, roof-to-floor convergence sensor assembly.

convergence in the center of the 7 development gate entry system was 3.3 in. Significant roof-to-floor convergence of 2.9 in between the tail yield pillar and the abutment pillar was measured prior to the abutment pillar bumps.

As was the case in 7 development, the roof-to-floor convergence was uniform and minor across the 8 development gate entry system until the mining of panel S-7 was adjacent to the instrumentation (fig. 37A). When the distance from the face position reached 500 ft, the failure of the head yield pillar coincided with entry closure of over 7 in adjacent to the abutment pillar. The stable 120-ft-wide abutment pillars fractured the bottom on their panel S-7 gob side. The increase in confined core size of the 8 development abutment pillars did not allow the roof to tilt toward the panel S-7 gob. This is reflected at the 500-ft distance from the face position by both the coalbed stress change data (fig. 23A) and the roof-to-floor convergence data (fig. 37A).

The majority of the crosscuts between the 120-ft-wide abutment pillars experienced approximately 1 in of convergence during the mining of panel S-7, and visually displayed no bottom heave (fig. 16F). However, the last 15

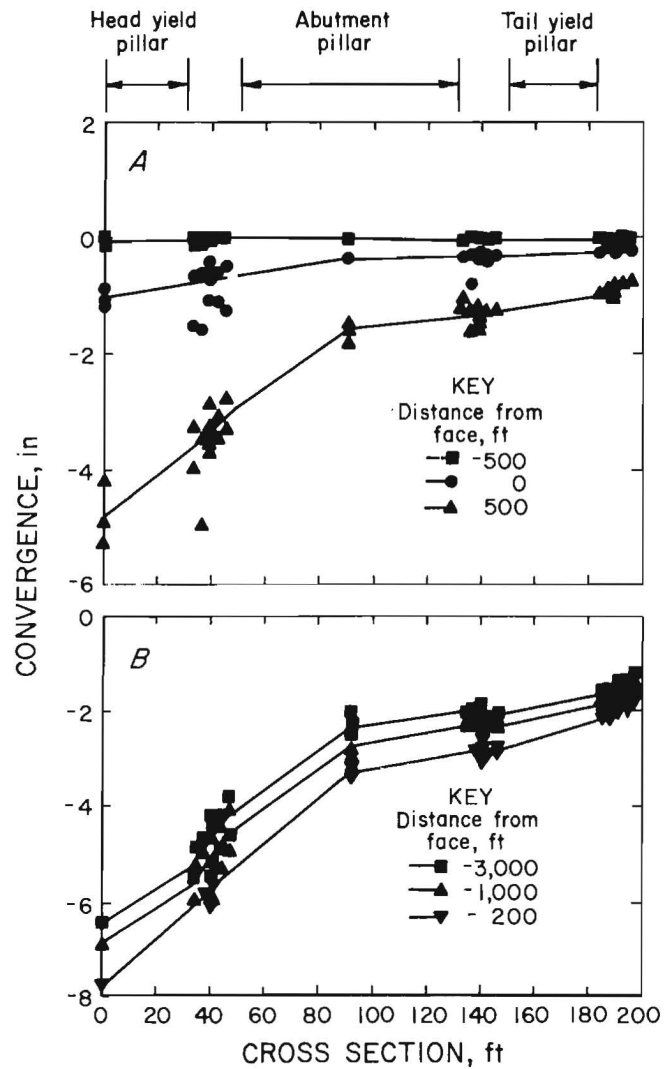


Figure 36.—Roof-to-floor convergence across 7 development cross section during mining of (A) panel S-6 and (B) panel S-7.

to 20 ft of the crosscuts on the panel S-7 gob side experienced bottom heave, which resulted in approximately 15 in of roof-to-floor convergence during the mining of panel S-7. These in-mine observations are reflected on figures 37A and 37B, at the 120-ft mark on the 8 development cross section.

Mining of panel S-8 up to the -1,000-ft distance from the instruments induced minor roof-to-floor convergence across the 8 development array, without significant roof tilt toward panel S-7 gob (fig. 37B). This situation changed upon the failure of the gob side of the 120-ft-wide abutment pillar, at the -200-ft distance from the face position (fig. 26). At this point 6.7 in of roof-to-floor convergence occurred at the center of the 120-ft-wide abutment pillar. The dashed line on figure 37B is a composite of in-mine observations and the roof-to-floor

convergence measurements. In-mine observations and convergence readings confirm the 120-ft-wide abutment pillar failure did allow the roof to tilt toward the panel S-7 gob, however, at a much later point in the tailgate pass than the 80-ft-wide abutment pillars in the 7 development gate entry system.

**Immediate Roof and Floor Strata Separation**

The reaction of the roof and floor strata to mining was evaluated through the use of multipoint extensometers to measure roof separation and floor heave. The 10- point

extensometers were located near the center of the 8 development array (fig. 18). The mining of panels S-7 and S-8 induced near-negligible roof separation over the first 25 ft of the mine roof. A total of only 0.125 in of separation was present at the -200-ft distance from the face position during the extraction of panel S-8 (fig. 38A). This is remarkable in light of the approximately 7 in of roof-to-floor convergence measured at this point, but it is believable because of the composition of the roof (fig. 38A).

The mining of panel S-7 induced only 0.122 in of bottom heave, as demonstrated by the -3,000-ft distance from the face position during the mining of panel S-8 (fig. 38B). Thus, a maximum of 0.25 in of the total 1.44 in of roof-to-floor convergence measured at that point (fig. 37A) is due to associated strata bed separation. This results in 1.19 in of entry closure that could be assumed to be the deformation of the abutment pillar. At the -200-ft face position of panel S-8 extraction, a maximum of 3.67 in of the 7-in roof-to-floor convergence is due to bed separation. This results in 3.33 in of entry closure that could be assumed to be the deformation of the abutment pillar at near-peak loading.

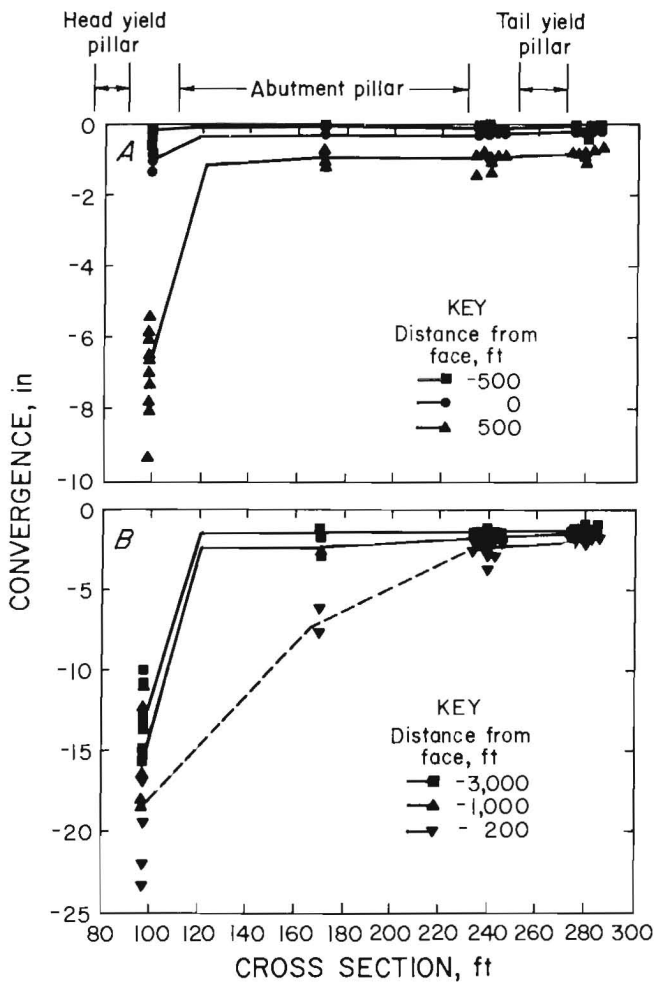


Figure 37.—Roof-to-floor convergence across 8 development cross section during mining of (A) panel S-7 and (B) panel S-8.

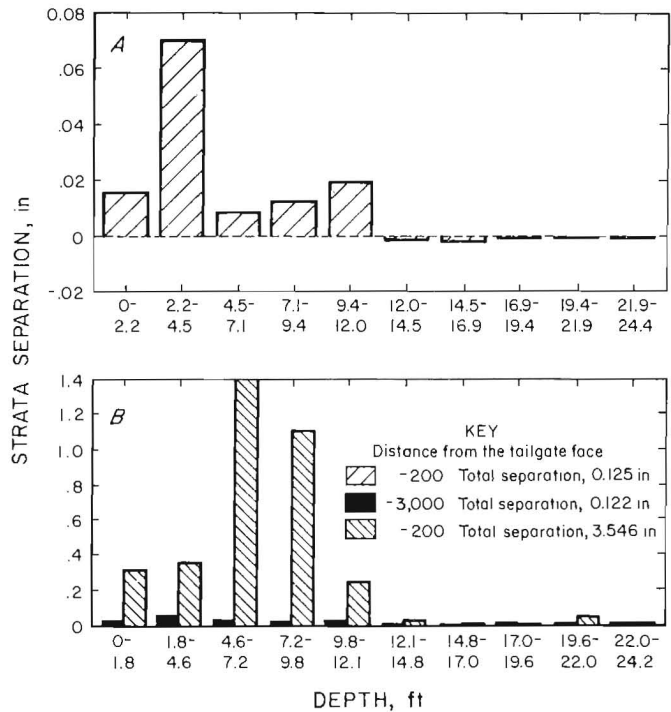


Figure 38.—Roof separation (A) and bottom heave (B) induced in center of 8 development instrument array.

## SUMMARY AND CONCLUSIONS

The Bureau evaluated two different, conventional long-wall gate entry configurations in a bump-prone coal mine in the Southern Appalachian Basin. The effect of the two designs on gate entry stability and bump occurrence was evaluated through two detailed instrument arrays, rock properties testing, and in-mine observations. The state-of-the-art instrumentation arrays utilized in the two detailed study areas consisted of stainless steel BPF's for indicating changes in pillar stress, coal extensometers for measuring pillar dilation, convergence stations for measuring roof-to-floor closure, a differential roof-sag indicator, and a differential floor-heave indicator. A permissible data acquisition system was employed to read coalbed stress and roof-to-floor convergence instrumentation in hazardous areas.

The original gate entry system (7 development) employed a 218-ft-wide yield-abutment-lead configuration with 30- by 80-ft yield pillars on either side of 80-ft-square abutment pillars. The new 238-ft-wide design (8 development) consisted of 20- by 80-ft yield pillars on either side of 120- by 180-ft abutment pillars. The new design requires less entry to be mined to advance the entire section, which generates an improvement through reduced mining requirements. However, leaving a larger pillar in the gob slightly decreases the extraction ratio. Continuous miner coal production rates were not affected by the design change.

Coalbed stress change data revealed that the yield pillars in both designs reached their ultimate strength during the headgate pass. The walls of broken coal formed by the tail yield pillars effectively shield workers from coal thrown in the event the center tailgate abutment pillars bump during the subsequent tailgate pass.

Roof-to-floor convergence and coalbed stress change data effectively isolated the timing of abutment pillar failure in both gate entry system designs. The 80-ft-square tailgate abutment pillars within the original gate system study area experienced structural failure 1,000 ft in advance of mining, and began bumping 500 ft in advance of the longwall face. This violent failure of the tailgate abutment pillars resulted in load transfer to the mined panel and the occurrence of bumps on the tailgate corner of the longwall face. The 120- by 180-ft tailgate abutment pillars within the new gate entry system study area did not

experience structural failure until 200 ft in advance of mining and did not bump until they were approximately 100 ft behind the face. Furthermore, bump intensity was greatly diminished with the larger abutment pillar system. Thus, the new design effectively shielded the tailgate corner of the mined panel from the excess loads that resulted in the face bumps with the original design.

The average weighted change in headgate abutment pillar stress induced by the headgate pass was approximately 6,000 psi for both designs, indicating that the design change did not produce a dramatic difference in pillar behavior. However, the yielding of the inner core of the 120- by 180-ft tailgate abutment pillars occurred considerably after the yielding of 80-ft-square tailgate abutment pillars. The larger abutment pillars did not reach their ultimate strength until the mining of the tailgate pass was 200 ft away from the instrumentation lines.

Coal extensometers demonstrated that the abutment pillars of both designs formed a 12- to 15-ft-wide yielded perimeter zone. The coalbed stress change data place the depth of the yield zone at 15 ft. The width of the yield zone in Pocahontas No. 3 Coalbed pillars at ultimate strength is concluded to be 15 ft, which does not significantly change when the two-dimensional size is increased. However, dramatic changes in coalbed thickness could alter the depth of the yield zone. Therefore, any increase in pillar size results in a direct increase in confined core size. Based on the 15-ft-wide confinement zone, the ratio of maximum stress core area to original pillar area for the 80-ft-square and 120- by 180-ft abutment pillars is 0.39 and 0.63, respectively. This 62-pct increase in functional bearing area per foot of gate entry length reduced abutment pillar stress and deformation, prevented excessive load transfer to the tailgate corner of the mined panel, and successfully eliminated the face bumps that were experienced with the original gate entry design.

This analysis of instrumentation response, combined with in-mine observations, has increased the understanding of high-stress gate entry pillar and longwall panel edge behavior. The insight into what determines the ultimate strength of coal pillars and the effect of yield zone confinement at ultimate pillar strength has advanced the current knowledge base on longwall gate entry system design.

## REFERENCES

1. Rice, G. S. Bumps in Coal Mines of the Cumberland Field, Kentucky and Virginia—Causes and Remedy. BuMines RI 3267, 1935, 36 pp.
2. Holland, C. T., and E. Thomas. Coal-Mine Bumps: Some Aspects of Occurrence, Cause, and Control. BuMines B 535, 1954, 37 pp.
3. Talman, W. G., and J. L. Schroder, Jr. Control of Mountain Bumps in the Pocahontas No. 4 Seam. Trans. AIME, 1958, pp. 888-891.
4. Wang, F. D., W. A. Skelly, and J. Wolgamott. In-Situ Coal Pillar Strength Study (contract H0242022, CO Sch. Mines). BuMines OFR 107-79, 1976, 243 pp.
5. Campoli, A. A., C. A. Kertis, and C. A. Goode. Coal Mine Bumps: Five Case Studies in the Eastern United States. BuMines IC 9149, 1987, 34 pp.
6. Campoli, A. A., D. C. Oyler, and F. E. Chase. Performance of a Novel Bump Control Pillar Extracting Technique During Room-and-Pillar Retreat Coal Mining. BuMines RI 9240, 1989, 40 pp.
7. Condon, J. L., and R. D. Munson. Microseismic Monitoring of Mountain Bumps and Bounces: A Case Study. Paper in Proceedings of the Sixth International Conference on Ground Control in Mining. WV Univ., 1987, pp. 1-9.
8. Iannacchione, A. T. Behavior of a Coal Pillar Prone To Burst in the Southern Appalachian Basin of the United States. Paper in Pre-Printed Papers, Second International Symposium of Rockbursts and Seismicity in Mines (Minneapolis, MN, June 8-10, 1988). Univ. MN, 1988, pp. 427-439.
9. Mark, C. Longwall Pillar Design—Some New Developments. Soc. Min. Eng. AIME preprint 89-103, 1989, 9 pp.
10. Hooker, V. E., and C. F. Johnson. Near-Surface Horizontal Stresses Including the Effects of Rock Anisotropy. BuMines RI 7224, 1969, 29 pp.
11. Agapito, J. F. T., S. J. Mitchell, M. P. Hardy, and W. N. Hoskins. Determination of In-Situ Horizontal Rock Stress in Both a Mine-Wide and District-Wide Basis (contract J0285020, Tosco Res., Inc.). BuMines OFR 143-80, 1980, 175 pp.; NTIS PB B1-139735.
12. Oyler, D. C., A. A. Campoli, and F. E. Chase. Factors Influencing the Occurrence of Coal Pillar Bumps at the 9-Right Section of the Olga Mine. Paper in Proceedings of the Sixth International Conference on Ground Control in Mining. WV Univ., 1987, pp. 10-17.
13. Ferm, J. C., and G. A. Weisenfluh. Cored Rocks of the Southern Appalachian Coal Fields. Univ. KY (Lexington), 1981, 112 pp.
14. Iannacchione, A. T., A. A. Campoli, and D. C. Oyler. Fundamental Studies of Coal Mine Bumps in the Eastern United States. Paper in Rock Mechanics, ed. by I. Farmer, J. J. K. Daemen, C. S. Desai, C. E. Glass, and S. P. Newman. Balkema, 1987, pp. 1063-1072.
15. Gauna, M., H. E. Hamilton, and B. R. Pothini. Practical Rock Mechanics for Safety and Productivity Improvements. Paper in Proceedings of the 7th International Conference on Ground Control in Mining (Morgantown, WV, Aug. 3-5, 1988). WV Univ., 1988, pp. 126-136.
16. Heasley, K. A., and K. Barron. A Case Study of Gate Pillar Response to Longwall Mining in Bump Prone Strata. Paper in Proceedings of Longwall USA (Pittsburgh, PA, Sept. 13-15, 1988). Maclean-Hunter (Chicago), 1988, pp. 92-105.
17. Campoli, A. A., and K. A. Heasley. Coal Mine Bump Research: Providing Tools for Rational Longwall Design. Proceedings of the 23rd International Conference of Safety in Mines Research Institutes (Washington, DC, Sept. 11-15, 1989). BuMines OFR 27-89, 1989, pp. 666-676.
18. Heasley, K. A. Understanding the Hydraulic Pressure Cell. Paper in Rock Mechanics as a Guide for Efficient Utilization of Natural Resources, ed. by A. W. Khair (Proc. 30th U.S. Symp. on Rock Mech., Morgantown, WV, June 18-23, 1989). Balkema, 1989, pp. 485-492.

## APPENDIX.—DATA ACQUISITION SYSTEM DESCRIPTION AND OPERATION

The Mini-Dan<sup>1</sup> is a data acquisition system developed by Mine Safety Appliances (MSA), primarily as a warning, alarm, and control system for use in mines and other permissible areas. The system is designed for real-time monitoring of the safety of environmental conditions; conditions out of the acceptable range must be immediately noted by a human operator and corrected. For this purpose the system has little need for a sophisticated data recording system, but it is important for readings out of normal range to be printed along with warning and alarm messages for documentation purposes. The Bureau's data acquisition requirements were for a system that could operate for long periods of time unattended and record all readings in a compact form. The original Mini-Dan system could record data only by sending it to a line printer. A later modification made by MSA especially for the Bureau allowed storage of data on hard disk.

<sup>1</sup>Reference to specific products does not imply endorsement by the U.S. Bureau of Mines.

The Mini-Dan is similar to most other data acquisition systems, in that it requires sensors, power, telemetry, and a data storage system. Since it is a data acquisition system for use in permissible areas, an additional requirement is for barriers to protect against the possibility of the system's causing a spark. The major components of the Mini-Dan system are listed, and their locations shown, in a block diagram format in figure A-1. The system is designed for use with a variety of sensors and control relays, but the sensors used by the Bureau were purchased from vendors other than MSA and were modified for use with the Mini-Dan system. The Mine Safety and Health Administration (MSHA) has set up a specific procedure for obtaining approvals, known as classifications, for sensors used with minewide monitoring systems. This procedure allows new sensors to be added to existing data acquisition systems relatively easily.

Signals from the sensors, either 0- to 1-V dc, 0- to 5-V dc, or 4- to 20-mA output, are sent to a voltage-to-frequency (V-F) conversion card (fig. A-2). The signal is

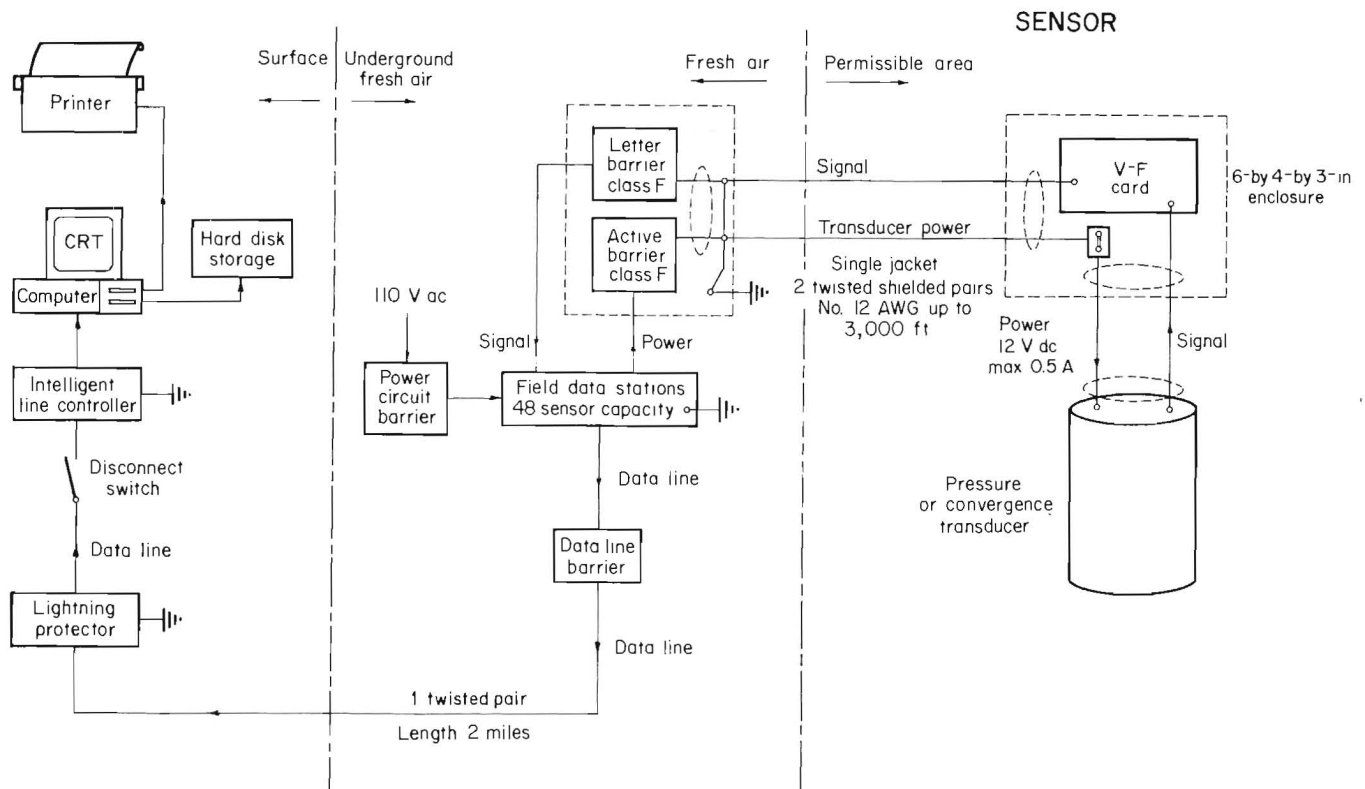


Figure A-1.—Data acquisition system configuration.

converted by this card from one of the above signal types to a low-voltage, 4,443- to 9,328- Hz frequency signal. The MSA system allows the transmission of analog signals, but frequency signals were chosen for long-distance data transmission to prevent the problems associated with cable voltage drops. The frequency signal is then transmitted from the sensor location to an outstation or field data station (FDS), where the barriers, power supply, and multiplexing electronics are located. A separate cable is required between each sensor and the FDS. Each cable contains two pairs of shielded twisted wires; of a minimum 19 gauge, 18-gauge wire was used. The signal pair also provides a 12-V dc supply to operate the V-F card. The second pair of wires to the sensor location provides a 12-V dc power supply to operate the sensor. The V-F card and sensor cannot be driven by a single power supply because the power supply to the V-F card is regulated such that connecting the sensor to it would drop the supplied voltage below the 6 to 7 V dc required to operate a V-F card. The V-F card is mounted within a 6- by 4- by 3-in enclosure [National Electrical Manufacturers Association (NEMA) Type 4], where the cable-to-sensor connections are also made. The enclosure is large enough to allow an additional circuit board to be installed in the case of the convergence sensors. At the other end of the cable, in a fresh air area, the signal pair is connected to a signal barrier and the sensor pair is connected to a power barrier. All barriers used by the Bureau with this system are class F barriers, but other classes could have been

used if required and the necessary sensor classifications applied for from MSHA.

The FDS is located in fresh air in a stable and safe underground area (fig. A-3). Each FDS requires its own separate 110- or 220-V ac power supply, and a power barrier between it and the mine power. The FDS unit contains the multiplexing circuitry, power supplies for the sensors, and the connections between the sensor cables and the cable to the surface. The FDS box used by the Bureau is specially configured by MSA for data acquisition. Typically an MSA FDS box is used to read data from eight carbon monoxide or methane analog devices and to operate eight relays. In the system used by the Bureau, 24 data channels are read and no relays are operated. This is within the capabilities of the FDS box, but the wiring harness is not set up to provide fuses and connections for all 24 channels. Special wiring harnesses are required to provide power and connections for all 24 channels operated by a single FDS box, and since the boxes are originally configured for no more than eight channels, three analog channels operate off each sensor power supply. If the fuse from any one sensor channel blows out, it interrupts power to three sensors. Data from each sensor are sent to an option board, which then sends them to the multiplexer board. The option boards can handle up to eight channels, and an FDS box can support up to three option boards.

Each FDS unit has its own address, and the Mini-Dan system may have up to four FDS boxes. The data sent to the surface from all four FDS boxes of a Mini-Dan system



**Figure A-2.—Underground examination of voltage-to-frequency card, attached to transducer-equipped borehole platened flatjack.**



**Figure A-3.—Underground examination of field data station and associated equipment.**

are transmitted over a single, minimum 19-gauge twisted pair, which may be several miles in length. The signal sent to the surface is a series of 12-V dc pulses and includes the data from each sensor, FDS status information, and an identifier for that FDS unit. The data transmitted for each channel are in the form of an 8-bit word, which limits the resolution of the Mini-Dan system at the computer to 1 part in 256 or roughly 0.5 pct. The resolution of the frequency signal to the FDS unit is better than 1 part in 4,000 or about 0.02 pct. A barrier is also required at the FDS on the signal line. The data line must be connected to the surface through a lightning arrestor and a disconnect switch.

The data line is connected to a modem, which calls the operating FDS units, interprets the signals from them, and sends the data to the computer containing the Mini-Dan operating programs. The Mini-Dan operating programs allow for organization of data on screen and printed pages, for calibration of the sensor output, and in the case of the modified Bureau Mini-Dan system, for data to be sent to storage on a hard disk. The readings from any sensor may be placed on any page or multiple times on a single page, giving a flexible screen output. Readings from the sensors are updated every few seconds. However, the system allows pages of sensor data to be printed only once per day or once per hour, and the entire page must be sent. The data sent to the hard disk is exactly the same text or ASCII file sent to the printer, including all spaces, etc. This results in data files that take up a large amount of disk storage and require a great deal of editing before they can be effectively used.

The Bureau is using two sensors with the Mini-Dan system, pressure transmitters to read BPF's and a string potentiometer to measure convergence. Neither of these sensors is available from MSA, so it was necessary to find sensors compatible with the Mini-Dan system, and to obtain a classification from MSHA for each sensor.

The pressure transmitter chosen was a strain gauge type of device manufactured by T-Hydrionics. The transmitter is excited by a nominal 12-V dc supply and provides a 0- to 5-V dc output signal, proportional to the pressure as long as the excitation voltage is between 9.5 and 14 V dc. At excitations below 9.5 V dc the sensor output is no longer regulated, but for a given excitation voltage (down to 1.4 V dc; below an excitation of 1.4 V dc the transmitter provides no output), the output voltage is proportional to the pressure. The 0- to 5-V dc output signal is compatible with one of the three output signals accepted by the MSA V-F card. The transmitter can be configured for pressure ranges of 0 to 10,000, 0 to 20,000, or 0 to 30,000 psi, depending upon the way the sensing diaphragm in the sensor is machined and upon the unit calibration. The same electronic circuit can be classified for all three pressure ranges. The Bureau permit requires the use of the MSA V-F card. However, T-Hydrionics has independently obtained a classification from MSHA for the pressure transmitter.

The convergence sensor is a string pot type of potentiometer. Several manufacturers make such devices, which provide a 0- to 500-ohm output resistance, depending upon the extension of a wire. A number of extension ranges are also available, from 2 to 2,000 in. Because of the 0.5-pct resolution of the Mini-Dan system, the greater the range of the sensor used, the poorer the resolution. Any convenient excitation and output voltage may be used with these devices. A simple voltage regulator circuit was added inside the NEMA enclosure to convert the nominal 12-V dc MSA input voltage, which usually varied after cable voltage drops from between 11.1 and 11.5 V dc at the sensor to a 5-V dc input to the potentiometer. Since the lowest commonly available voltage regulator output is 5 V dc, this was chosen as the sensor output voltage range. The sensor classified by MSHA in this case was the string potentiometer, a voltage regulator circuit, and the MSA V-F circuit board.